

# Design of a flexible hollow hinge for a cryogenic environment

MSc. Thesis

E.J. Klomp

**UNIVERSITY OF TWENTE.**

Mechanical Engineering  
Department of Precision Engineering  
Enschede

Thesis committee

Chairman:	Prof.dr.ir. D.M. Brouwer
Supervisors:	Dr.ir. M. Nijenhuis Dr. M.A. Lewińska-Maresca
	Ing. J.W. Kragt
External members:	Dr.ir. G.M. Bonnema

September 30, 2021

# PREFACE

Before you lies the results of my MSc thesis 'Design of a flexible hollow hinge for a cryogenic environment'. The research has been commissioned by Astron Nova and is carried out within the Department of Precision Engineering. This thesis is the final assignment of the Mechanical Engineering Master's education. The assignment was performed in 8 months and will be concluded with this report, a presentation and an oral exam. The completion of these three components will mark the end of my studies. During the courses of this thesis, the COVID-19 (Coronavirus) spread in the Netherlands, resulting in urgent advice to work from home.

Firstly, I would like to thank my daily supervisor, Marijn Nijenhuis, for his guidance and for understanding my challenges in completing this thesis working from home. You were always ready to help me when I got stuck on a problem or if I had an issue with the software.

Secondly, I want to thank the rest of my supervisors, Dannis Brouwer, Mirka Maresca, Jan Kragt and Marijn Versteeg, for all their advice and for providing a different perspective.

Lastly, I would like to thank all the people who have helped me to find motivation by creating a workspace outside my room and providing me with feedback.

Eline Klomp  
Enschede, September 2021

# ABSTRACT

Flexure hinges are a common solutions for smooth and accurate control of a movement. In this research, a hollow flexure hinge is designed for the rotation of a triple mirror system for an instrument of the European Larges Telescope (ELT). The study aims to maximizing the deflection of a one degree of freedom system, while maintaining high second and higher term natural frequencies (vibration modes). The flexures are developed using the Freedom and Constraint Topologies (FACT) theory, and optimized with multibody software Spacar. Multiple concepts have been developed of which three were selected for detailed analysis. During the de-

velopment of the concepts, the use of tapered flexures is analyzed with the use of Finite Element Method (FEM) software Ansys Workbench. The study showed that even though the geometry of flexure hinges can rotate at a large angle, the vibration modes and stress still limit the maximum rotation angle. With the use of tapered flexures foreshortening (shorting) issues can be prevented and stress can be reduced. The optimizations show that the three leaf spring torsion model can be rotated by an angle of seven degrees around the z-axis while fulfilling all the other requirements. Additional study will be needed in order to enlarge the maximum rotation angle.

# CONTENTS

<b>Preface</b>	<b>1</b>
<b>Abstract</b>	<b>2</b>
<b>1 Introduction</b>	<b>5</b>
1.1 Background . . . . .	5
1.2 Nova . . . . .	5
1.3 Assignment . . . . .	5
1.4 Scope . . . . .	6
1.5 Process . . . . .	6
<b>2 Theory</b>	<b>7</b>
2.1 Degree of freedom (DoF) . . . . .	7
2.2 Existing flexures . . . . .	7
2.3 FACT . . . . .	7
2.3.1 Maxwell's contribution . . . . .	7
2.3.2 Blanding's contributions . . . . .	7
2.3.3 Constraint lines for the hollow flexure . . . . .	8
2.4 Flexures . . . . .	8
2.5 Multibody dynamics . . . . .	8
<b>3 Requirements</b>	<b>10</b>
3.1 Design challenges . . . . .	10
<b>4 Concept development</b>	<b>11</b>
4.1 Concepts . . . . .	11
4.2 Optimization . . . . .	12
4.3 Design comparison . . . . .	12
4.3.1 Results . . . . .	13
4.4 Conclusion . . . . .	13
<b>5 Concept 1</b>	<b>16</b>
5.1 Volume expansion . . . . .	16
5.2 Final design . . . . .	17
5.3 Production . . . . .	17
5.4 Conclusion . . . . .	18
<b>6 Butterfly</b>	<b>19</b>
6.1 Final design . . . . .	19
6.2 Volume expansion . . . . .	20
6.3 Conclusion . . . . .	20
<b>7 3 leaf spring torsion concept</b>	<b>21</b>
7.1 Foreshortening . . . . .	21
7.2 FEM analysis . . . . .	21
7.2.1 Tapered system . . . . .	25
7.3 Final design . . . . .	25
7.4 Conclusion . . . . .	26

<b>8 Discussion, Conclusion and recommendations</b>	<b>27</b>
8.1 Discussion and conclusion . . . . .	27
8.2 Recommendations . . . . .	28
<b>References</b>	<b>29</b>
<b>A Existing flexures</b>	<b>30</b>
<b>B FACT</b>	<b>33</b>
<b>C List of concepts</b>	<b>34</b>
<b>D Concept optimization</b>	<b>43</b>
D.1 Results of the optimization of the concepts . . . . .	43
<b>E Concept 1</b>	<b>50</b>
E.1 Optimization configuration . . . . .	50
<b>F 3 leaf spring torsion concept</b>	<b>51</b>
F.1 Comparison between the different method of tapering . . . . .	51

# 1 INTRODUCTION

## 1.1 Background

A flexible joint, or flexure, is a solid structure that can bend in a specified direction while remaining stiff in the other directions. Flexure hinges are used to transmit loads between two components while keeping control of the motions of the (entire) system [1]. A leaf spring is an example of a flexure. A flexure enables the designer to produce the product out of one piece of material while retaining the same degree of freedom (DoF). For hundreds of years flexures have been used in precision instruments [2] and are still used in today's applications like optical systems, micro-robots, clean room equipment and many more. However, the use of a hollow flexure is a new approach. In terms of manufacturing and operational characteristics, flexures have advantages over conventional joints. Flexures are typically manufactured monolithically, out of one single piece of material, which avoids assembly errors, and potentially leads to a more compact design. Conventional joints work on the mechanism of sliding or rolling of two bodies, while flexures rely on the elasticity of the material [3]. Therefore flexible joints have the operational advantages of little friction losses and no need for lubrication. This provides smooth displacements without backlash, hysteresis or (friction) wear [2][3]. Besides the operational and manufacturing advantages, the absence of hysteresis of the material makes the structure useful for precision design, vacuum space or a cryogenic environment [3].

Besides all these advantages there are also some downsides to flexures. The main disadvantage is the limited range of motion. While a conventional joint has an infinite range of motion, flexures have not. The range of motion can be altered by the thickness of the material, but it will still be limited [2][3]. A second challenge, is the multi-axial loading; a conventional joint will be rigid in all directions except for one direction, while flexures have (relative) high stiffness in the direction in which motion is undesired and are compliant in the desired direction [2][3][4]. A third disadvantage can be that coupled flexure systems will become non-linear when prescribing a trajectory un-

der active control which makes the design more complex than for conventional joints [5]. The last disadvantage of flexures is the low resistance to fatigue, due to cyclic loading throughout the flexure life span, little cracks can appear in the material and weaken the structure [4].

## 1.2 Nova

Nova (for who this study is done) is a company designing instrumentation for the extremely large Telescope (ELT), which is the largest optical/near-infrared telescope in the world with four instrumentation's: HARMONI, MICADO, MAORY and METIS [6]. Nova is a collaboration of four Dutch universities that work together on the Dutch Astronomical agenda [7], with the main office located in Leiden. Nova consists of different departments, with the Optical IR instrumentation group in charge of the development, production and testing of the next-generation astronomical instruments. This team works together with Astron (Dwingeloo).

## 1.3 Assignment

This study focuses on the METIS instrumentation. METIS looks at the infrared light emitted by stars and galaxies. Therefore, the instrument is placed in a cryogenic environment (vacuum space with a temperature of  $-200^{\circ}C$ ). Because of the large size of the telescope, and its instruments, METIS will be used in a fixed configuration. As a consequence, the instrument sees a sequence of rotating images of the sky, which need to be "derotated" in order to compare the measurements. To overcome this problem Nova-Astron is designing a highly accurate 3-mirror derotator mechanism, Figure 1.1, located inside a cryogenic environment. This derotator mechanism needs to be rotated during the measurement to account for the rotation of the earth. This study is on designing a flexible hinge solution to rotate the 3-mirrors inside a cryogenic environment to compensate the rotation of the earth. The flexure requires one (rotational) DoF and a hollow inside of  $\varnothing 100mm$  for the optical bundle to pass through.

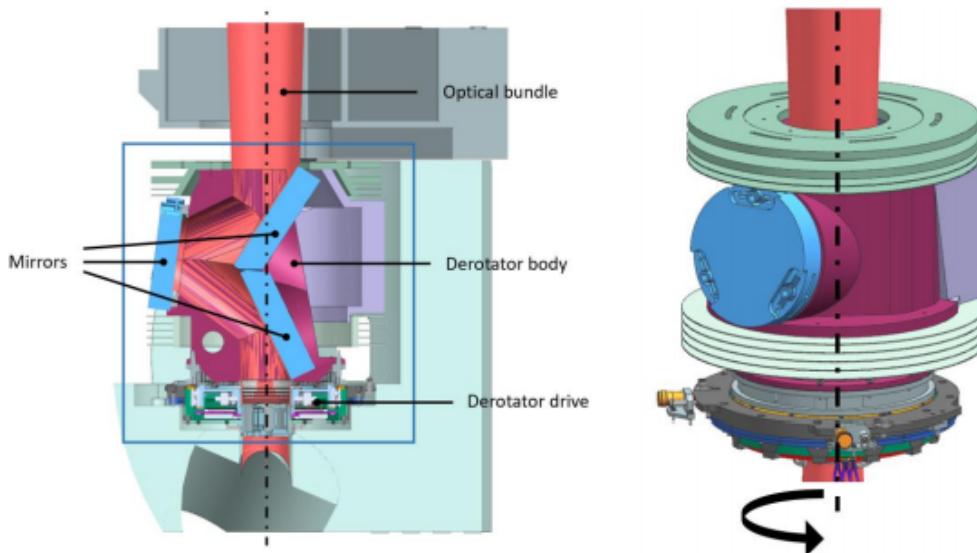


Figure 1.1: On the left a view within METIS, on the right the outside along with the derotation direction

#### 1.4 Scope

The focus of the study is on designing a hollow flexure with one DoF (rotation around the z-axis) and a large rotation range ( $22^\circ$  angles in both directions). The theory of Hopkins [8], Freedom and Constraint Topologies (FACT), and research into existing flexures, is used to create concepts. The developed concepts are optimized with multi-body software, Spacar and when needed the finite element method (FEM) software Ansys Workbench. The stress and vibration modes (natural frequency) are considered the most important requirements to compare the concepts, followed by the maximum rotation angle.

#### 1.5 Process

The design process, pictured in Figure 1.2, starts with the determination of a general idea with FACT. Then, with the guidance of the requirements, a starting configuration is made. This system is modelled in Spacar with the corresponding relations between the bodies and the fixed world. Spacar is used to examine the possibility of fabrication via an understanding of the design parameters and execution faults. This is measured by the stress, motion and vibration modes. By re-designing the concepts, different values can be measured and the difference between the concept properties and the requirements can be reduced. Finally, a single concept is chosen, and a scale model is manufactured.

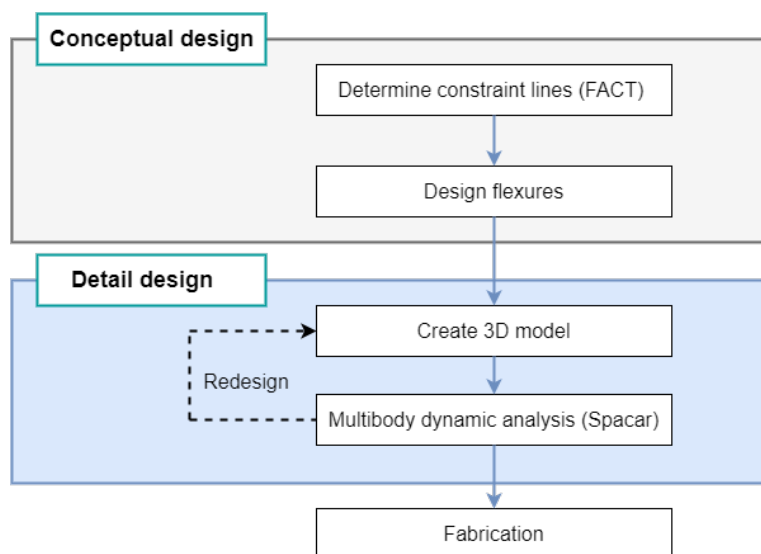


Figure 1.2: Overview of the design method

## 2 THEORY

This chapter will elaborate on the relevant theories for the design of the flexures. Firstly the needed DoF is discussed, followed by the FACT method, which is used during the design process. The different kinds of flexures used and their corresponding constraint lines are discussed. Finally, the multibody dynamics and the software used in the optimization is explained.

### 2.1 Degree of freedom (DoF)

METIS consists of three tilted mirrors which will deflect the infrared waves so the imaging will be flat and the different results can be compared. While METIS is doing observations, the earth is slowly spinning. Therefore, the mirrors need to rotate at the same speed of the earth during the measurements. This results into a system with 1 DoF, namely a rotation around the z-axis. In Figure 2.1, a schematic image of METIS is given. Here it can be seen that the middle axes, rigidly connected to the mirrors, need to rotate around the z-axis while the other directions are fixed. The designed flexures need to have 5 constraints to uphold all the fixed directions between the fixed world and the mirrors, and also support the load of the mirrors.

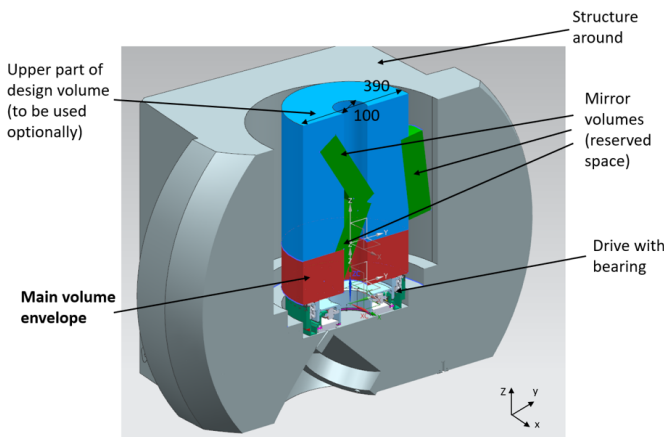


Figure 2.1: Schematic view of METIS with in red the volumes for the hollow flexure

### 2.2 Existing flexures

As mentioned in the introduction, the use of flexures is not new and there exists multiple one DoF solutions. In Table A.1 (Appendix A) a list of the most common rotational flexures shown. These flexures are not (yet) hollow but could be altered to have a hollow center.

### 2.3 FACT

FACT is a method to design (parallel) flexure systems. According to Hopkins [8], a designer only needs to know the number of DoF and their directions to know every possible design solution for a (parallel) flexure system. The FACT method uses the principle of constraint-based design: Maxwell's and Blanding's contributions.

#### 2.3.1 Maxwell's contribution

James Clerk Maxwell formulated a relationship between the number of constraints and DoF, seen in equation 2.1 where  $N$  are the non-redundant constraints and  $R$  the DoF [9]. Every free-standing object has 6 DoF in a three-dimensional space, 3 translations and 3 rotations. For every non-redundant constraint added to the system, one DoF will be removed. When  $R$  is equal to zero the system will be fully fixed.

$$6 - N = R \quad (2.1)$$

#### 2.3.2 Blanding's contributions

Blanding's research has shown that a constraint can be seen as a line which is infinitely stiff in the length direction, but is compliant in every other direction [10]. He also observed that not only the constraint could be seen as lines, but the DoF can be seen as rotations around lines, called the freedom lines. He stated that a translation can be modelled as a rotation in a perpendicular direction at an infinite distance, Figure 2.2. Blanding's Rule of Complementary Patterns gives the relation between constraints and DoF used by FACT, which

is 'Every freedom line intersects every constraint line'[8]. So the freedom line(s) can be determined by finding the line(s) intersecting every constraint line and vice versa. The power of this rule is that it provides a method for both analysis and design, by converting between complementary freedom and constraint line patterns.

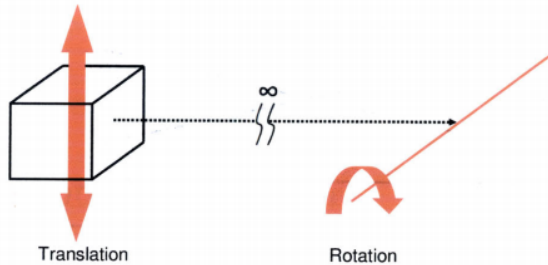


Figure 2.2: Rotational freedom line of a free translation [10]

### 2.3.3 Constraint lines for the hollow flexure

When designing a system for a given set of DoF, the most appropriate case from FACT can be selected. Consequently, enough non-redundant constraints. By repeating this process multiple times, all the possible parallel systems can be designed.

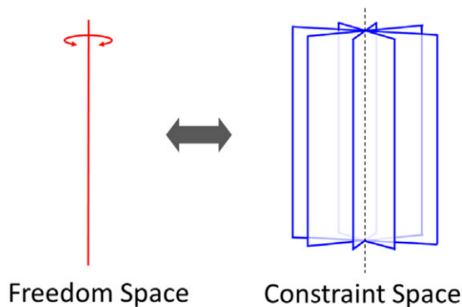


Figure 2.3: Case 1, type 1 [8]

For this research the case shown in Figure 2.3 is used. Where the red line indicates rotation in the z-direction and 5 non-redundant constraints need to be selected for the blue planes. An overview of all the possible cases is showed in Appendix B.

## 2.4 Flexures

Although FACT shows the designer which constraint lines are needed for the desired movement, it does not provide information about the shape of the flexures, dimensions or even materials. The designer needs to determine those. In this report, there are two kinds of flexures used; leaf springs (3 constraints) and folded leaf springs (1 constraint). The constraint lines corresponding

with the flexures are shown in Figure 2.4 where the blue line shows the appurtenant constraint line(s) of the flexures. All the dimensions and material properties are further developed with multi-body dynamics.

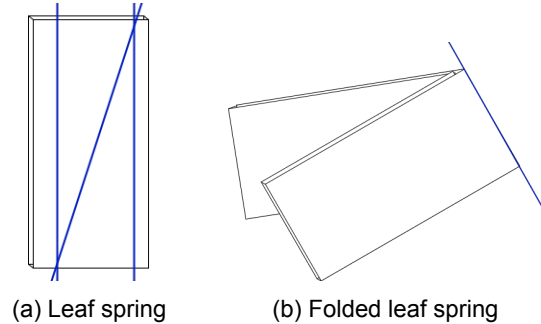


Figure 2.4: Two kinds of flexures with their constraint lines in blue

## 2.5 Multibody dynamics

A multibody system consists of rigid bodies connected by flexible (beam) bodies, which can move relative to each other, see Figure 2.5 (where the joints/hinges restrict the movements) [11]. There are two methods for multibody analysis; Kinematic analysis (uses constraints and DoF) and Dynamic Analysis (Newton-Euler equations). These methods are used to explore the relationship between body motions and internal mechanical loads. Multibody dynamics analysis was initially developed as a modelling tool for rigid multibody systems with simple tree-like topologies [12]. Nowadays, the tool can handle linearly and nonlinearly elastic multibody systems with arbitrary topologies. Consequently, it is a suitable fundamental design tool in many areas of engineering.

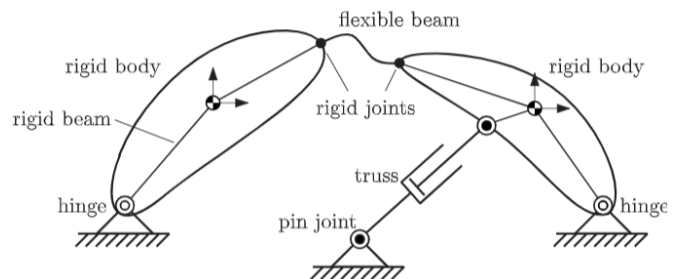


Figure 2.5: Flexible multibody system [11]

There are three main categories in multibody dynamic; rigid multibody, linearly elastic multibody systems and nonlinearly elastic multibody systems [12]. Where the first category consist of systems with only rigid bodies and the other two

are systems with rigid and flexible bodies. In this research, systems from the last two categories are discussed. In multibody dynamics, in general all bodies have a large motion and there is a large relative motion between the systems various components. This results in an inherently nonlinear problem. The terms “linearly” and “non-linearly elastic” used in the classification refer to the elastic behaviour of the bodies themselves. Linear elastic multibody systems have nonlinear dynamical equations of motion, although the representation of the elastic behaviour of the bodies could be linearized. In this research, a large angle is needed, but the permanent deformations remain limited. The systems used could be categorized as linear elastic multibody systems. To calculate the influence between the bodies and the nonlinear dynamic behaviour, software can be used to calculate the stress/strain, displacements and vibration modes of the system.

In this research, the software Spacar is used for the design of the concepts. In Spacar, a difference can be made between rigid and flexible bodies. Where the flexible bodies can have all 6 beam deformation modes (1: elongation, 2: torsion: 3 and 4: out-of-plane bending, 5 and 6: in-plane bending) or less and the rigid parts have no deformation modes. The different bodies can be connected to the fixed world, and/or a load can be added. So Spacar can determine the internal influences of the bodies, and the influences of the external forces on the performance of the system. The values generated by Spacar can be used in optimization, where a redesign of a system can led to negative or positive changes in the parameters. This provides the designer with an understanding of the behaviour of the multibody systems, and helps to generate the best concepts based on the initial constraint lines.

# 3 REQUIREMENTS

For the design of the flexure, the operating conditions at which the flexure should function are transferred to a set of requirements. The requirements are given a priority rating; where 3 means the requirement has to be fulfilled and 1 can be interpreted as a preference rather than an essential requirement. During the design process, this list is used to develop and evaluate the concepts.

## 3.1 Design challenges

As can be seen in Table 3.1 all the requirements are written to the best possible values. However, some requirements influence each other resulting to interesting challenges.

The flexure(s) will undergo multiple cycles and therefore it is necessary that the flexure(s) do not plastically deform during operation. The entire system will be in a cryogenic environment resulting in the material choice of Aluminum 6061 – T6. This material has been used and tested in this environment before. Consequently, the material properties are well-known. For the maximum stress allowed in the flexure, the yield tensile

stress at –200 degree Celsius is taken, therefore no permanent deformation will occur. A way of keep the stress low is to have a relatively thin flexure. However, a low thickness leads to low vibration modes. A challenge is created in designing a flexure that will have both low stress and a high second vibration mode.

Besides the stress and vibration mode, the large angle will also present issues. Flexures are mostly used for small precise angels. Because of the requirement for having an angle of 22.5 degrees in both directions, the system can become unstable, or have high (internal) stresses.

A final challenge is the mass of 90 Kg located above the flexure. Although the gravity axis aligns with the systems middle axis it will influence the flexures significantly. In order to prevent deformation of the flexures due to the gravitational force, the thickness has to be sufficiently high. The large mass provides a parabolic response of the stress due to a reduction in thickness, instead of a linear response. This can lead to a counter intuitive responses of the flexure(s).

Table 3.1: Requirements

Priority	Objective
3	The system needs to have a open centre to allow the optical beam to go through the flexure
3	The flexure must be able to move a least a mass of 90kg located 0.266 m above the origin of the flexure
3	The flexure needs to operate in a cryogenic environment (67K)
3	The stress needs to be below the yield tensile stress of the material (in this study below the 324 MPa)
3	All vibration modes generating an undesired movement needs to be above 30Hz (natural frequency)
3	Decentering of the midpoint of the system has to be lower than 0.1mm
3	The system has 1 degree of freedom (rotation around the z-axis)
3	The flexure needs to hold for 200.000 cycles (18 years)
2	The system needs to fit in the given volume of 390mm outer ring, 100mm inner ring, 133mm height
2	The flexure needs to rotate 22,5 degree (0.393 rad) in both directions around the z-axis
1	Gravity axis needs to be aligned with the optical beam

# 4 CONCEPT DEVELOPMENT

In this chapter the concepts are discussed as well as the optimization method and a reduction of the number of concept is done.

to be 5 non-redundant constraint lines. This results in a list of concepts (a selection is explained below, see Figure 4.1).

## 4.1 Concepts

With the use of the FACT method, different scenarios of constraint lines were determined. Because the system is a one DoF system there need

Figure 4.1a to 4.1c consist of two leaf springs, each have 3 constraint lines, which are connected to the fixed world at the outer sides of the leaf springs. This system has one overconstraint in the z-direction of the system.

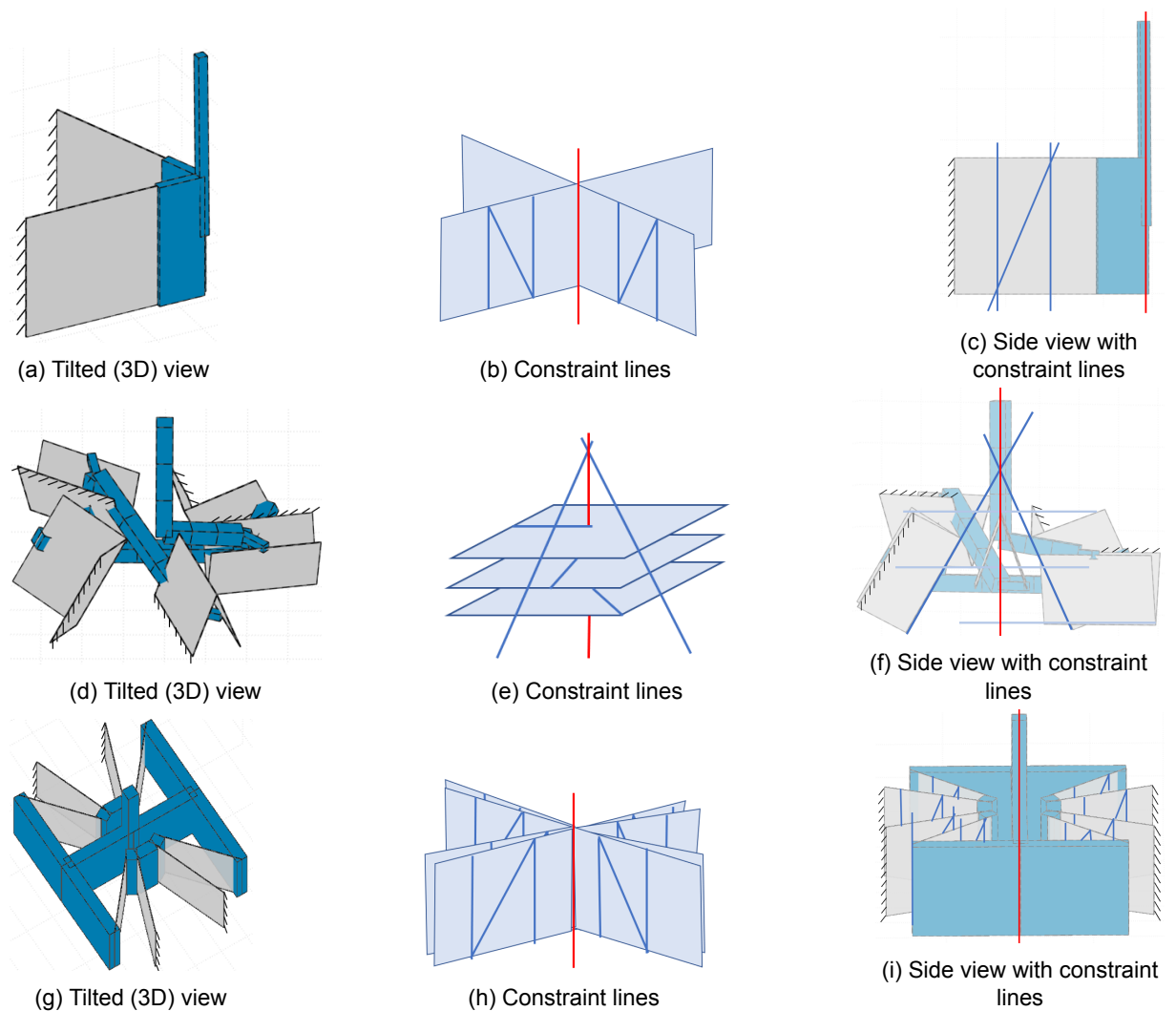


Figure 4.1: A selection of concepts where the blue parts are rigid and the grey parts flexures

Figure 4.1d to 4.1f, this concept has 2 angled and 3 horizontal constraint lines. The two angled constraint lines intersect at a point on the middle axis, which will become the rotation axis. This system has no overconstraints.

Beside the FACT method some concepts are a redesign of existing flexures. The problem with the existing flexures is that they do not have a hollow middle for the optical beam. One concept inspired by the Butterfly hinge is depicted in Figure 4.1g to 4.1i.

The concepts in Figure 4.1 are used as a base for different concepts. More concepts are developed by changing the constrain lines position, or by adding extra flexures. A full overview of all the concepts is depicted in Appendix C.

## 4.2 Optimization

For comparison of the different concepts, all the concepts are optimized with respect to the stress. Stress has been chosen as a baseline because of the requirement's priority, and since alterations to the parameters have a direct response in stress. While the other properties have less flexibility to optimize to certain value. By optimizing stress, it is possible to visualise the differences in angles and the vibration modes of the concepts.

The stress levels of almost all concepts are far above the maximum stress when a maximum rotation of  $\pm 22.5$  degree ( $\pm 0.393$  rad) is considered. Consequently, it is difficult to state the differences and potentials of the concepts. Hence, the optimization has been performed for an maximum rotation of  $\pm 12.5$  degree ( $\pm 0.22$  rad).

## 4.3 Design comparison

The concepts have been compared on four properties:

- stress under an angle of  $\pm 0.22$  rad without warping influences;
- stress under an angle of  $\pm 0.22$  rad including warping effects;
- the vibration modes including warping effects;
- the rotation vectors.

The stress under an angle of  $\pm 0.22$  rad without the effects of warping needed to be as low as possible, but at least below the 324 MPa. A stress level below the maximum stress implies that the angle can be larger than the applied angle. This

is an advantage because the preferred rotation range is larger than the maximum rotation in the comparison.

In practise warping is a common effect. Warping occurs when the ends of a leaf spring are constrained and the system is loaded in torsion [13]. When a free end of a leaf spring is loaded with torsion the cross-section has a displacement distribution in the longitudinal direction, Figure 4.2. This derives from the distribution of shear stresses on the flexure, and damages the flatness of the cross-section, which is called warping. Warping also happens in a case of non-uniform torsion together with a large deformation, where the torsion moment varies over the length of the flexure. In these cases, a lateral force in the y-direction causes in-plane bending and shearing. This shearing can be significantly for flexures where  $w/l < 4$  [13], which is the case for many concepts. Warping can lead to an increase in stiffness and thus an increase in stress.

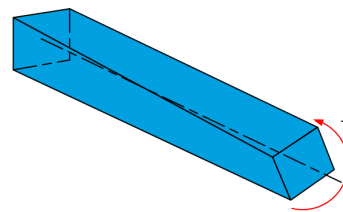


Figure 4.2: Schematic view on warping

To investigate the DoF of the system the vibration modes in different directions are evaluated. When flexures are used all moving directions have different stiffness. A movement is called free when the vibration mode is significantly low compared to the other modes. In the same way, high vibration modes lead to a stiff direction. Therefore, the first vibration mode of the concepts should be low and have at least a difference of 15 Hz with the second vibration mode to be considered one DoF. According to the requirements, the preferred difference between the first and second vibration mode is 30 Hz.

The final requirement for comparison are the rotation vectors (no parasitic motion, Figure 4.3). When a leaf springs is bent the result can be a shortening of the flexure. Similarly, a flexure can bend in the x- or y-direction while being rotated around the z-axis. These are examples of why a rotational movement is not always a pure movement. To find the parasitic motion, the rotation vectors are compared. A pure rotation will be zero in x- and y- direction and one in the z-direction.

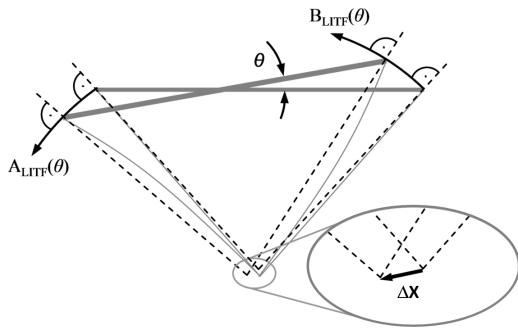


Figure 4.3: Parasitic motion where  $\Delta X$  is the undesired movement of the rotation point

#### 4.3.1 Results

The results of the concept analysis are shown in Figures 4.5, 4.6 and 4.7, where Figure 4.5 shows the stress analysis, Figure 4.6 the rotation vectors and Figure 4.7 the second vibration mode analysis. An entire overview is shown in Appendix D.1. Here, some observations are highlighted and explained.

Concerning, the four requirements, it is concluded that many concepts have problems with the vibration modes. This is caused by the small volume in which the flexure can be placed. A higher stiffness can be obtained when the constraint lines of the flexures are placed further apart. In the available volume for the flexure this is not possible. The consequence of the low difference in vibration modes is that the system moves in unwanted directions.

The requirement that the flexure should be able to hold a mass of 90 Kg, proves to be a challenge for multiple concepts. This mass is located above the flexures and generates a relatively large force on the system. This results in a certain minimum thickness in the flexures to prevent plastic deformation and limits stress reduction. In theory, the stress on a flexure can be reduced by decreasing the thickness of the flexures. A thinner flexure results in lower stress. However, the mass on the flexure requires a minimum thickness causing the stress to have a minimum possible value as well.

As shortly mentioned before, warping will happen when the height and width of a leaf spring are similar to each other or when the flexure is loaded with torque. This results in large changes in stress for the model with the effects of warping.

For a rotational movement leaf springs will bend. The bending of a leaf spring will cause shortening of the length of the flexure (Figure 4.4). This loss in length results in an extra force pulling the middle to the side (the red arrow). When the

flexures are spread out in the volume these extra forces will work in opposite directions creating large internal stresses. This is indicated via the high stress levels in the symmetric concepts.

The vibration modes of the flexure are depending on the rotation of the flexure. Therefore, the second vibration mode is evaluated over the full rotation range of the flexure. The results are shown in Figure 4.7a and 4.7b. From those Figures, it can be concluded that none of the concepts have good vibration modes at the maximum rotation angle. When the line tangents are compared it can be seen that the Butterfly and Concept 3.2 have the lowest decrease in vibration modes during the movement.

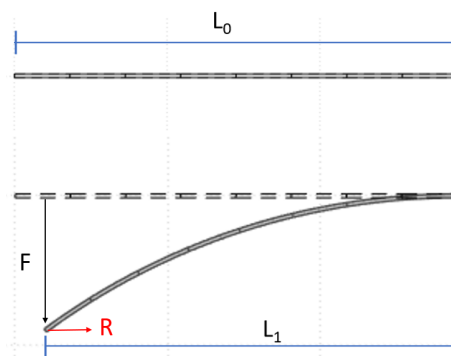


Figure 4.4: Shorting due to bending.  $F$  is the bending force and  $R$  is the force due to shorting

#### 4.4 Conclusion

The evaluation of the analysed concepts with respect to the four main requirements leads to the conclusion that three concepts score the best. These concepts are the Butterfly, Concept 1 and the 3 leaf springs torsion concept. All three of these concepts have a pure rotation (Figure 4.6). The Butterfly has the lowest stress, which shows a promising option for a bigger angle. The Butterfly also show distinct difference between first and second vibration modes when warping is considered.

The 3 leaf springs torsion concept has acceptable stress levels when warping is not considered but performs much less when warping is taken into account. However, the vibration modes show the biggest difference between the first and second modes.

Furthermore, Concept 1 also has good stress level without warping and has the lowest increase in stress due to warping compared to the other concepts. At the same time, the vibration modes are not yet at the desired differences nevertheless they do fulfil the 15 Hz limit.

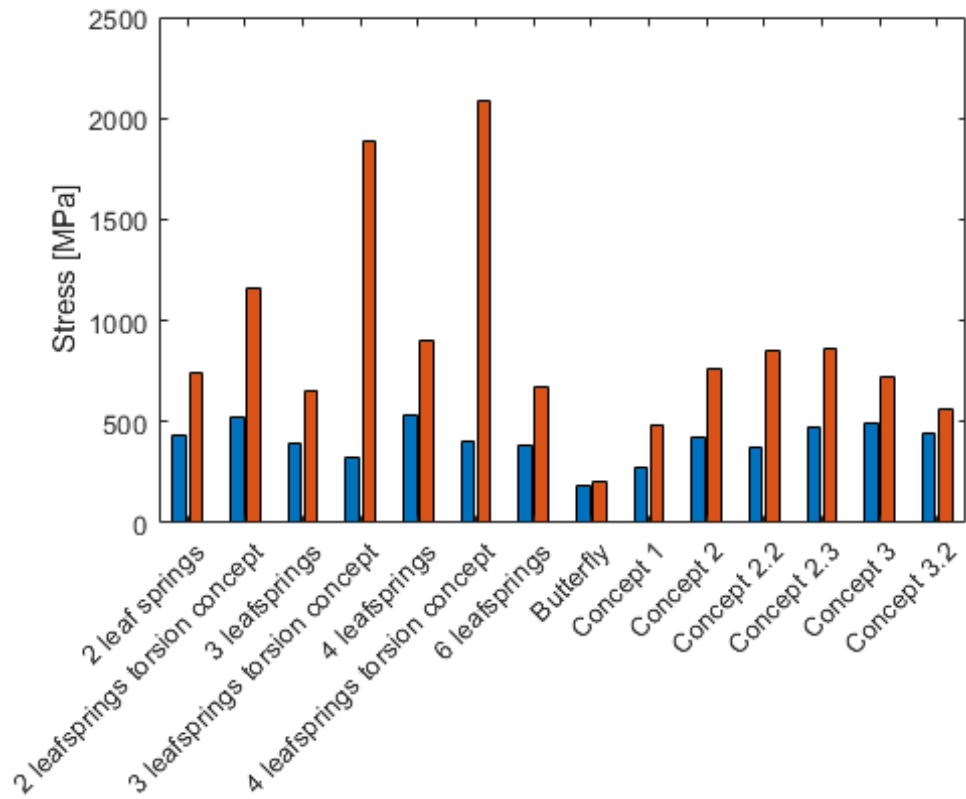


Figure 4.5: Stress results for a rotation of 0.22 rad. The blue bars are the stress excl. warping and the red bars are the stress incl. warping

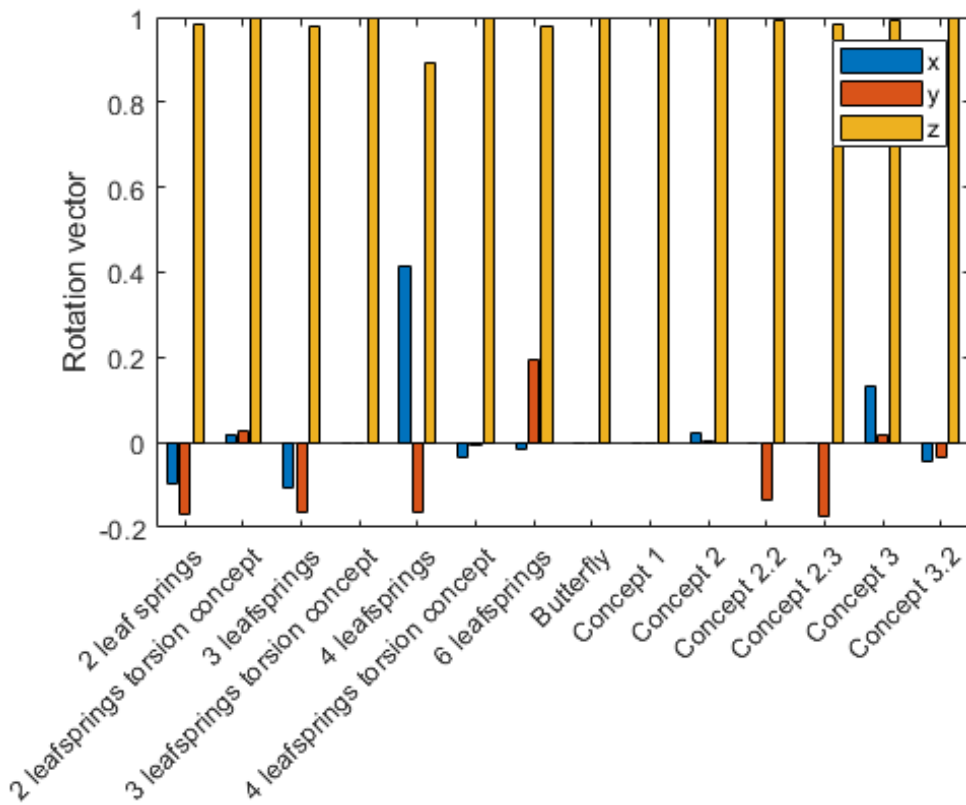
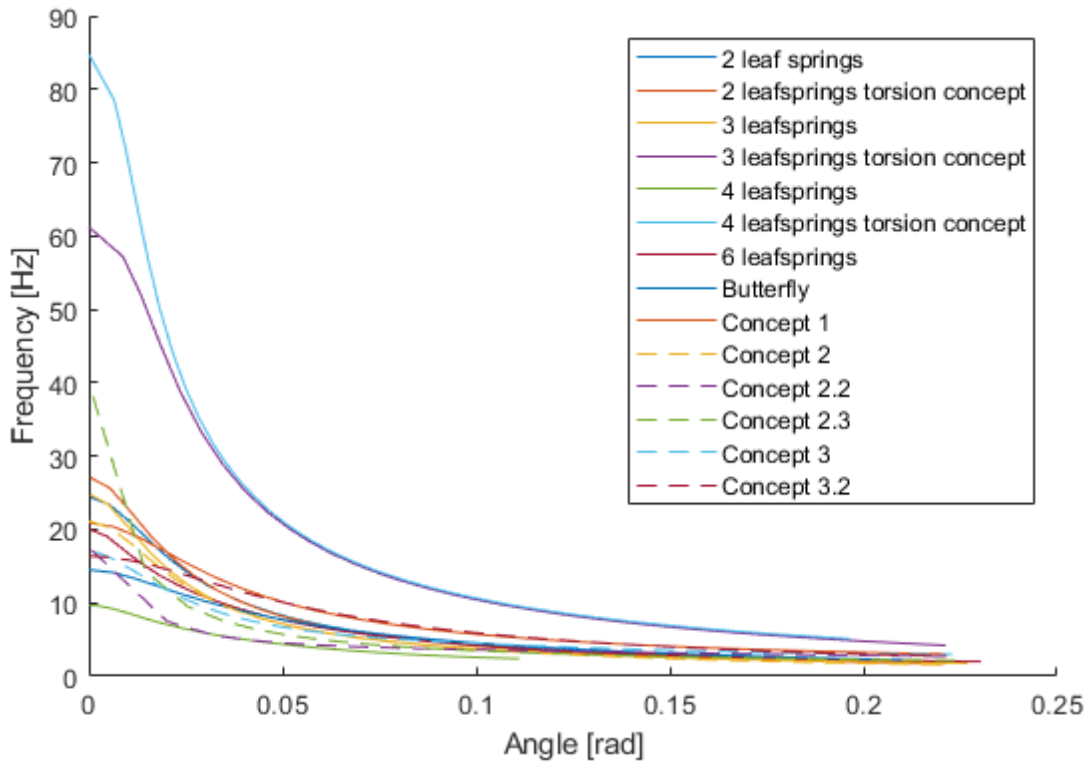
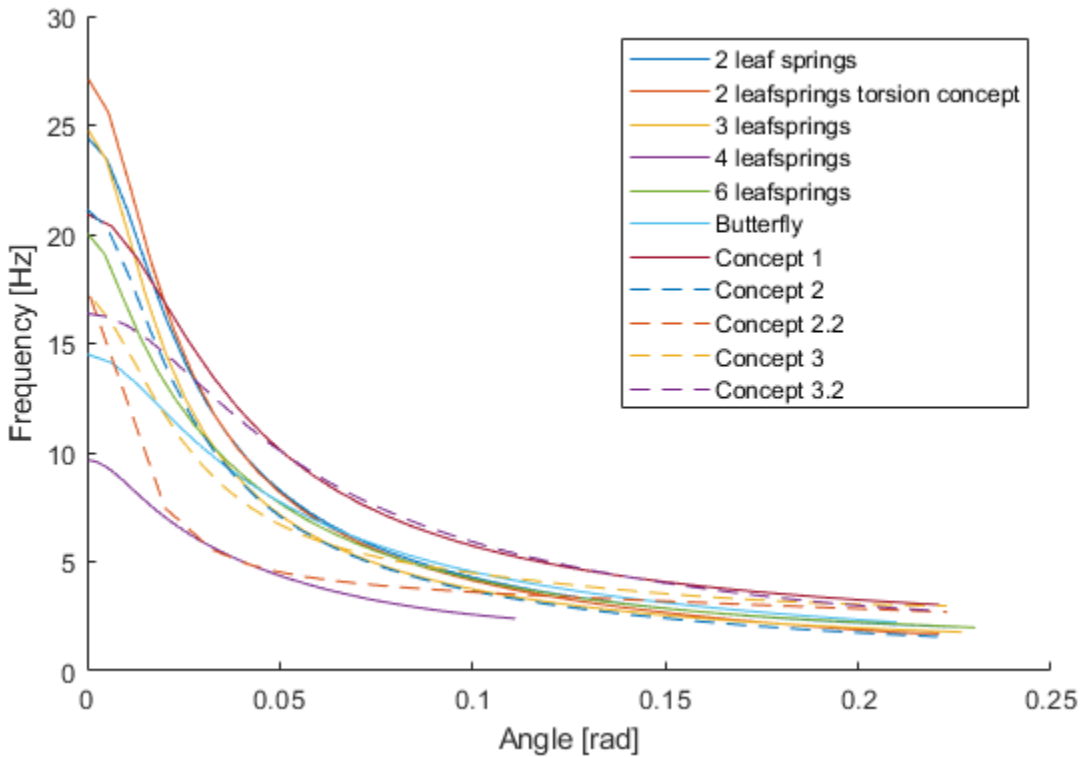


Figure 4.6: Result of the rotation vectors of the concepts



(a) Second vibration mode of all concepts



(b) Second vibration mode of part of concepts

Figure 4.7: Second vibration mode throughout a rotation around z

## 5 CONCEPT 1

From the evaluation of the concepts after the preliminary optimization Concept 1 (Figure 5.1) shows good potential. In this chapter, the concept is developed further by exploring the benefits of 10% and/or 20% extra volume. Following the final design and production technique is discussed.

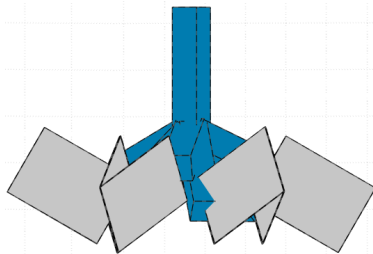


Figure 5.1: Concept 1

### 5.1 Volume expansion

In the preliminary optimization is found that Concept 1 has a pure bending moment around the z-axis (Figure 5.2), but the requirements of stress and the vibration modes are not met. To improve the vibration modes, the rotation points (the two points where three of the constraint lines intersect) must be placed further apart, therefore a large volume is needed. A study to the benefits of extra volume is performed with an increase of 10% and 20% in height and/or width relative to the initial volume. From the results can be concluded that the vibration modes indeed benefit from extra height. The stress did not improve from the extra height, as it stayed around 400 MPa. Only adding more width to the system had a negative influence on both the stress and vibration modes.

This is the case because extra width doesn't allow the rotation points to be further apart, while it does allow larger flexures which are more prone to warping and buckling.

For the maximum volume (20% more height and width) an optimization with two variables is performed. The first variable is the angles between the legs of the folded leaf springs, called  $\alpha$ . The second is the angle between the folded leaf springs and the horizontal middle axis of the system, called  $\gamma$ . The results on the stress analysis are depicted in Figure 5.3. Figure 5.3 shows that the stress is lowest when the flexures are almost horizontal (constraint lines pointing in the z-direction) or vertical (constraint lines are in one plane in x and y). The low stress for the horizontal scenario comes from the fact that the rotation points are the furthest apart. The vertical case has low stress due to the influences of the angle on the height of the leaf spring, which results in less internal stresses caused by rotation of the leaf springs during bending.

The difference in angle  $\alpha$  in Figure 5.3 shows that for the stress it is beneficial to have a small angle between the two leaf springs. A bigger angle will have more resistance to bending than a smaller angle, resulting in higher stresses. The downside of a smaller angle between the leaf springs is lower natural frequencies. Therefore, a balance needs to be found where the natural frequencies uphold the desired vibration modes, but still have a small angle to maintain a low stress. The results of the vibration modes study are shown in Appendix E.

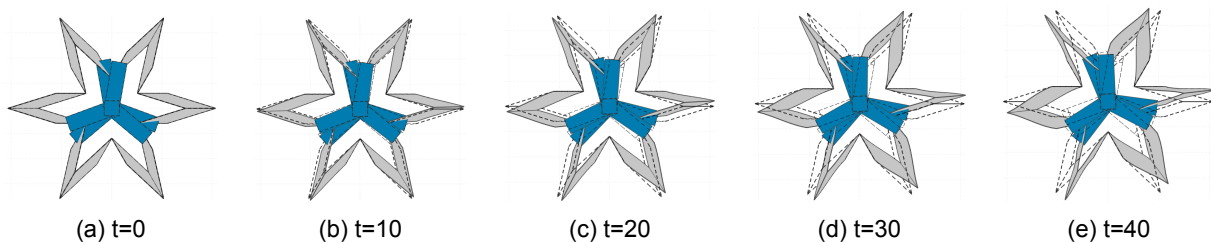


Figure 5.2: Desired movement of Concept 1 over time in top view

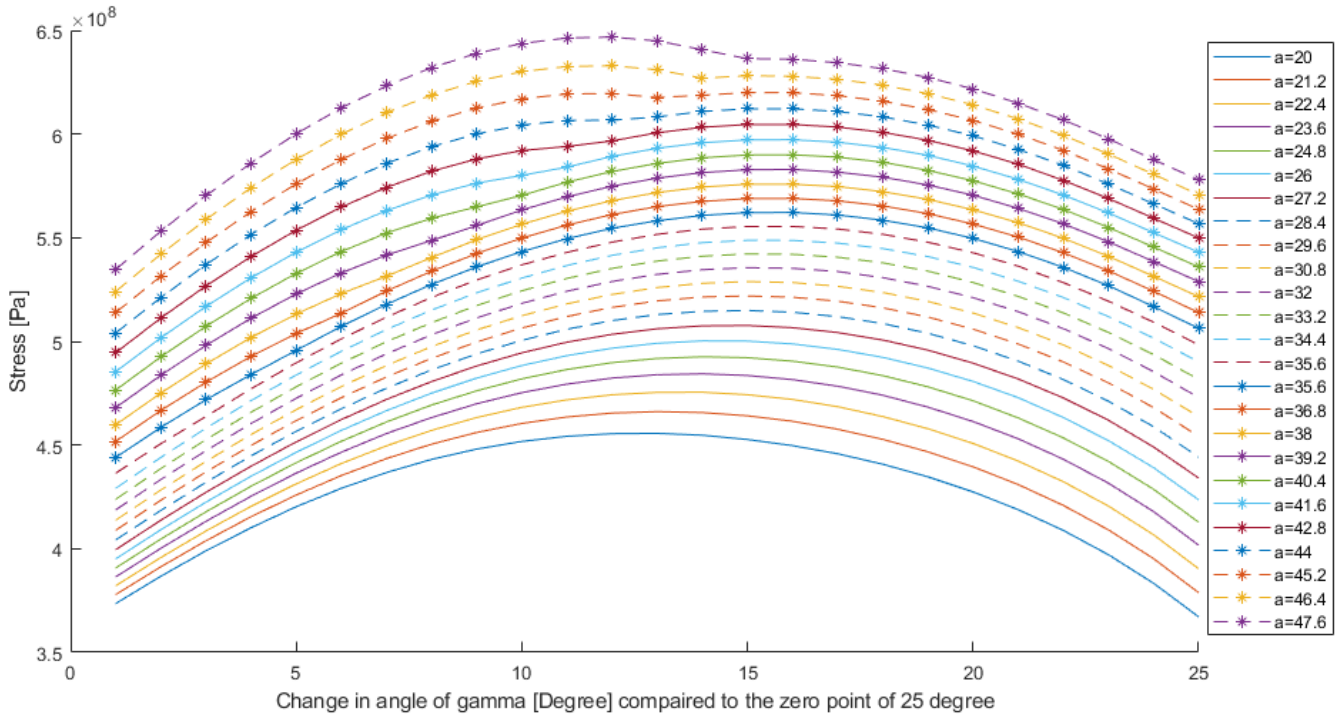


Figure 5.3: Stress optimization concept 1 where the x-axis shows the angle between the folded leaf spring and the middle axis where the zero points are 25 degrees and  $\alpha$  is the angle between the leaf springs

The analysis to increase the dimensions of the flexure show that there is no situation in which the stress and vibration modes fulfil the requirements when considering 20% more height and width for the flexure while still rotation a  $\pm 0.22$  rad angle. This can be seen in Figure 5.3 because the lowest point of the vertical axis is higher than the maximum allowed stress.

## 5.2 Final design

A configuration in which Concept 1 has low enough stress and also uphold the minimum vibration mode of 30 Hz while deforming a  $\pm 0.22$  rad angle, can be achieved with a volume increase of 50% in height and 30% in width. A possible configuration is shown in Figures 5.4 and 5.5.

If a volume of 20% more width and height is preferred it is also possible to stay under the max stress by reducing the angle. The stress and vibration mode have a linear response to the reduction of the thickness. To increase the second vibration mode a thicker flexure is needed. This will also result in an increase in stress, but on a smaller scale. Therefore, a thickness can be found where the stress and second vibration mode will be at the critical value around the same

angle. With 20% more volume, a thickness of 2 mm provides an angle of  $\pm 0.124$  rad ( $\pm 7$  degree) for maximum stress and 30 Hz throughout the movement. In Figures 5.6 and 5.7 this concepts is shown.

The system has to uphold 200.000 cycles within a life span of 18 years. To account for the fatigue of the material the maximal stress need to be 47% of the yield tensile stress, 151 MPa. This will reduce the maximum angle to  $\pm 0.069$  rad ( $\pm 4$  degrees), for the situation with 20% extra volume. The properties of this scenario are summed up in Table 5.1. If the system in the initial volume is used the maximum angle is even smaller ( $\pm 0.059$  rad or  $\pm 3.4$  degrees).

## 5.3 Production

Concept 1 is, a very compact design, inside the set volume. The combination of the angles of the flexures, and the limited space between the flexures results to a complicated production process. Nova Astron has an in-house production process for milling with a CNC machine, but for this hollow flexure concept, the clamping in the machines will be difficult to achieve. Possibly a different production technique need to be considered.

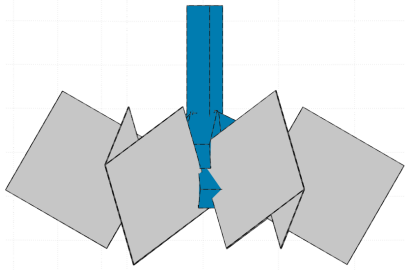


Figure 5.4: Final design concept 1 (50% more height and 30% more width)(side view)

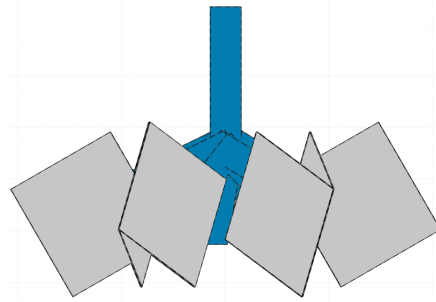


Figure 5.6: Final design concept 1 (20% more volume)(side view)

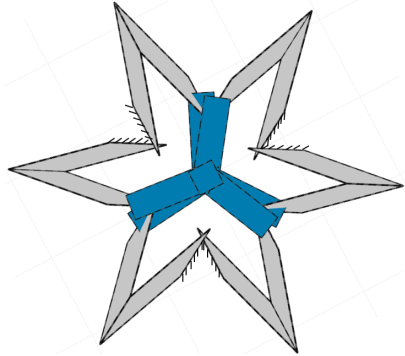


Figure 5.5: Final design concept 1 (50% more height and 30% more width)(top view)

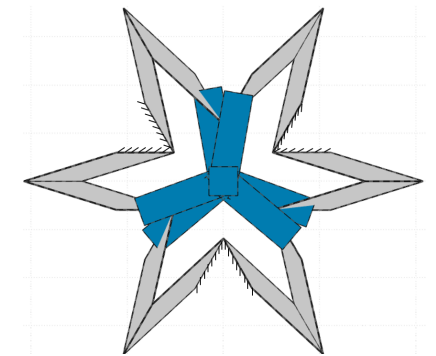


Figure 5.7: Final design concept 1 (20% more volume)(top view)

Table 5.1: Properties Concept 1 (20% more volume)

Thickness	Angle	Stress incl. warping	Vibration modes incl. warping
1.75 mm	$\pm 0.069 \text{ rad}$	150.880 MPa	1. 3.169 Hz 2. 33.94 Hz 3. 34.23 Hz

#### 5.4 Conclusion

After some optimization Concept 1 is able to rotate around the z-axis while obtaining good vibration modes throughout the movement. However, an angle of  $\pm 22.5$  degree cannot be achieved while staying below the maximum stress. When an 18

year life span is considered, with the initial volume Concept 1 can rotate  $\pm 3.4$  degree. When the height and width are increased by 20%, Concept 1 can rotate  $\pm 4$  degrees. For the production of this concept milling is a insufficient production technique, so an alternative solution needs to be found, which will result in higher costs.

# 6 BUTTERFLY

In this chapter the final design of the Butterfly is discussed as well as the influences of extra volume.

## 6.1 Final design

The Butterfly, discussed in Chapter 4.3, already fulfilled the stress requirement. However, the vibration modes were on the lower side (15 Hz for the second vibration mode). To increase the gap between the first and second vibration mode the two leaf springs connected to the fixed world (the flexures located in the middle) need to be under a larger angle from each other for the upper and lower case. This will result in an increase in stress and a higher second vibration mode. The new configuration is shown in Figure 6.1, the corresponding properties in Table 6.1 and the desired motion is shown in Figure 6.2. The distances between the flexures in series are just enough to achieve an angle of  $\pm 0.22$  rad. Nevertheless, for this project a larger angle is desired. To increase the angle the flexures in series need to be placed further apart, creating more space for the deflec-

tion. This results in a system that is more prone to rotation in the x-y plane, in other words, the second vibration mode will decrease. To detain the second vibration mode within the 30 Hz, the analysis showed that the angle cannot become larger than  $\pm 0.22$  rad.

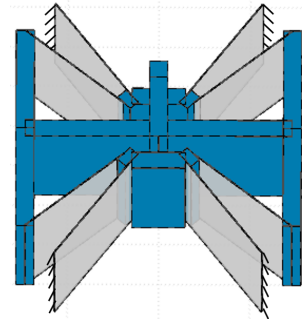


Figure 6.1: Final design Butterfly

The flat design of the Butterfly and large spaces between the components allows this concept to be manufactured with the preferred production technique of Nova Astron (milling).

Table 6.1: Properties Butterfly

Thickness	Angle	Stress incl. warping	Vibration modes incl. warping
1.07 mm	$\pm 0.22 \text{ rad}$	321.539 MPa	1. 1.15 Hz 2. 34.03 Hz 3. 34.59 Hz

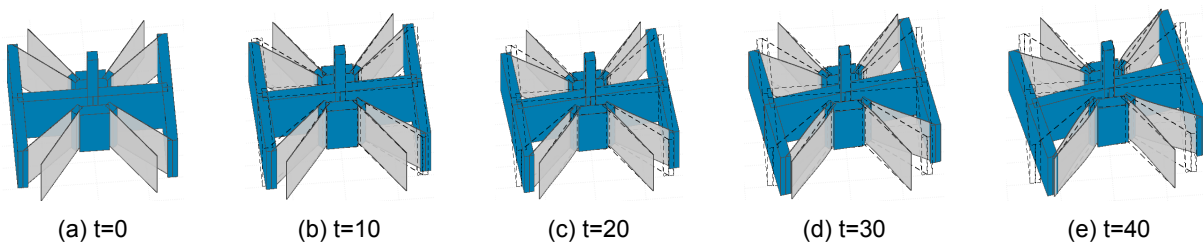


Figure 6.2: Desired movement of the Butterfly over time

## 6.2 Volume expansion

The final design of the Butterfly, fulfils the requirements at the beginning of the deformation. However, when the system is rotated the second vibration modes decrease (Figure 6.3). For a stable system, the second vibration mode needs to be at least 30 Hz throughout the movement, hence the benefits of extra volume is investigated. Therefore, an increase of 10% and 20% in height and/or width is analysed. In all cases, the stress decreases and is below the critical level, while a larger effect is visible on the vibration modes. When the thickness remains the same, extra height increases the vibration modes while the slope becomes steeper. When extra width is added, the vibration modes with a zero angle are lower compared to the initial volume, but they have similar slopes. A combination of extra height and width is desired to start at a higher vibration mode, while maintaining a lower decline. The stress remains low in all cases, so the influence of the thickness can be explored. For all volume cases, the thickness of the flexures is increased until the stress is just below the 324 MPa. By increasing the thickness, the vibration modes increase and as a result the flexure acts more inline with the requirements. The results of the vibration modes are shown in Figure 6.3.

The analysis shows that the flexures with an opti-

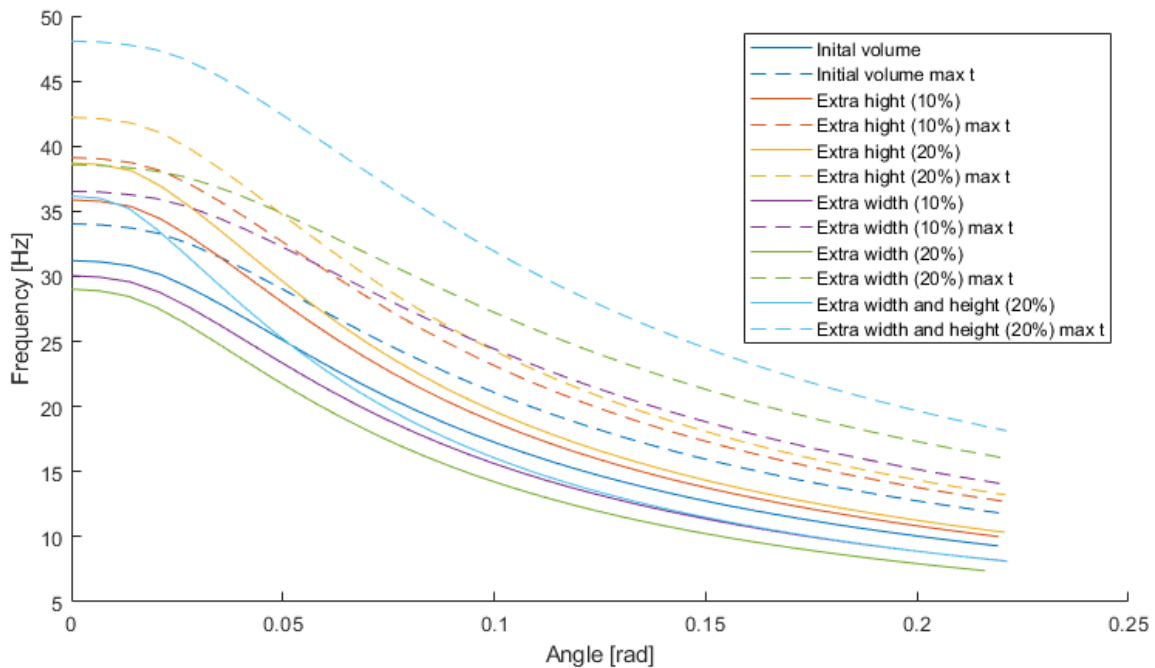


Figure 6.3: Second vibration mode through the rotation around z of the Butterfly with different volumes. The solid lines show the results of the flexures in different volumes but with the same thickness and the dashed lines show the results of the flexures in different volume with an optimized thicknesses

mized thickness, provides the highest frequency for the second vibration mode at rest, and with maximum rotation. However, even the largest expansion of 20% in height and width still results in a mode below 30 Hz. Indicating that for the stress and geometry a  $\pm 0.22$  rad deformation is possible, however only a  $\pm 0.125$  rad ( $\pm 7$  degrees) rotation can be done for the vibration modes. If a smaller volume is used the maximum rotation will be even smaller. To raise the vibration modes thicker flexure can be used, but then the stress will increase as well. For the case of 20% larger dimensions in height and width, a thickness of 2.2 mm will provides a rotation of  $\pm 0.178$  rad ( $\pm 10$  degree) in which the stress and vibration modes are both at their maximum allowed values.

Due to fatigue (as discussed in Chapter 5.2) the maximal angle will reduce to  $\pm 0.121$  rad ( $\pm 7$  degrees) for the case of 20% extra volume and  $\pm 0.1$  rad ( $\pm 5.7$  degrees) in the initial volume.

## 6.3 Conclusion

The Butterfly fulfils the stress, life span and vibration mode requirements when a maximum angle of  $\pm 7$  degrees is used with an increased in height and width of 20%. A maximum rotation of  $\pm 5.7$  degrees can be achieved with the initial dimensions. The concept can be made with milling which has the preference of the company.

# 7 3 LEAF SPRING TORSION CONCEPT

The 3 leaf spring torsion concept, Figure 7.1, fulfilled the important requirements after the preliminary optimization, however not all were met. In this chapter more analyses are done into stress reduction and the use of a series of flexures.

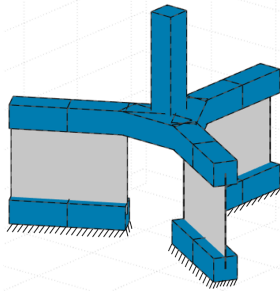


Figure 7.1: 3 leaf spring torsion concept

## 7.1 Foreshortening

In Chapter 4.3 it was discussed that warping has a large impact on the 3 leaf spring torsion concept. Part of this comes from the large almost square shape of the flexures, but the biggest impact is introduced by deformation difference along the flexures. When twisting a bar, the point which is the furthest away from the center has to deform more compared to a point closer to the central axis (see the deformation in Figure 7.2). This is called foreshortening and will lead to higher stress. A solution for this problem is the use of tapered flexures, Figure 7.3.

How large the tapering need to be can be determined by two methods [14], a parabolic shape for equal deflection in the z-direction or a conical shape for equal bending stress across the width

of the blades. The first method, the parabolic shape, can be determined by Equations 7.1 and 7.2. First, the values for  $\Delta y$  and  $\Delta z$  at maximum  $x$  need to be calculated. To maintain the same deflection,  $\Delta z$  needs to be the same for every point on the curve. Therefore, the length at  $x$  can be determined with Equation 7.3. If an angle of  $\pm 0.22$  rad is used  $\Delta z$  will be 8 mm.

$$\Delta y = (r + x)\Theta \quad (7.1)$$

$$\Delta z = 0.6 \frac{(\Delta y)^2}{L(x)} \quad (7.2)$$

$$L(x) = \frac{(r + x)^2}{(r + x_{max})^2} L(x_{max}) \quad (7.3)$$

For the second method, the conical shape, Equation 7.4 applies. Here  $\sigma_b$  is constant throughout the curve which leads to Equation 7.5 for calculation of the tapering of the flexures. Both methods are investigated further.

$$\sigma_b = \frac{3Et(r\theta)}{(L(x))^2} \quad (7.4)$$

$$L(x) = \sqrt{\frac{((r + x)\theta)}{((r + x_{max})\theta)}} L(x_{max}) \quad (7.5)$$

## 7.2 FEM analysis

The current software, Spacar, is not suited for tapered flexures, so Ansys Workbench is used for the analysis of the tapered leaf springs. For this analysis, the models are first built in Solidworks

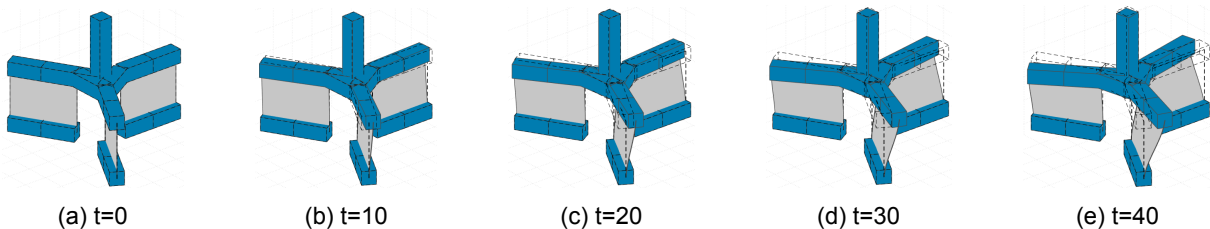


Figure 7.2: Desired movement of the 3 leaf spring torsion concept over time

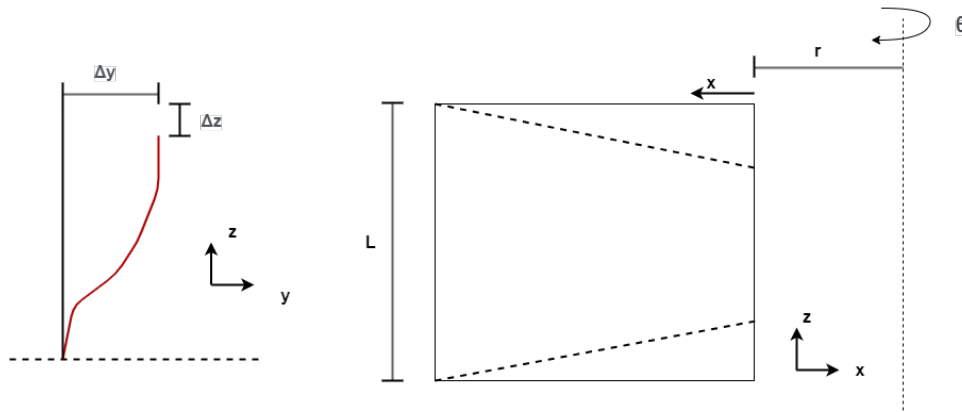


Figure 7.3: The concept of tapered leaf springs

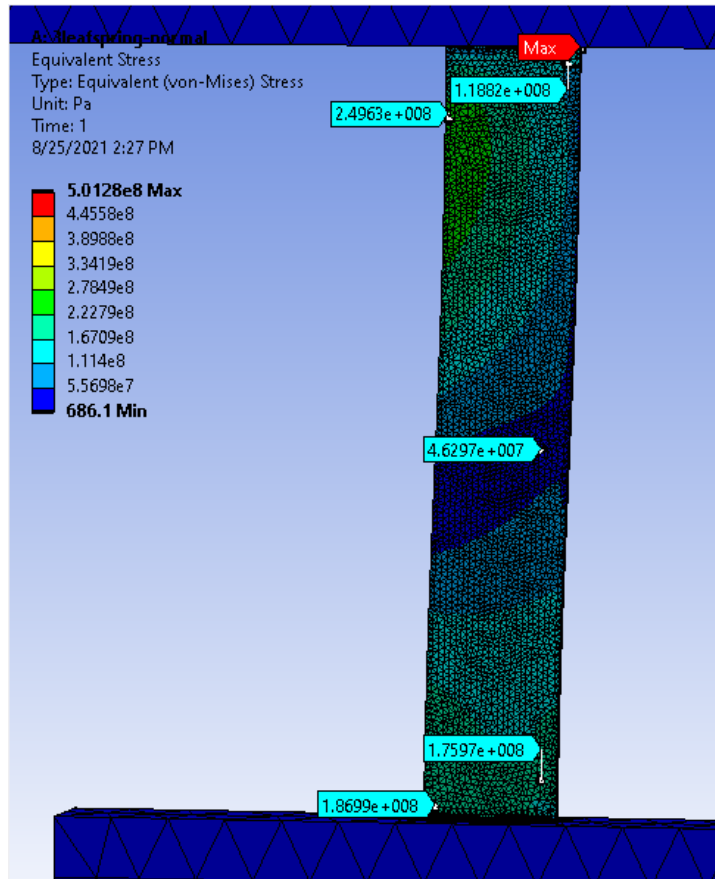
where the dimensions and configuration of bodies are similar to Spacar. Then, the models are transferred to the FEM software (Ansys Workbench) where the loads, fixes, materials and mass are added. The contact surfaces are connected with shared topologies. The results are obtained by the equivalent stress analysis. Firstly, the results of Spacar for the non tapered case are compared with Ansys Workbench to validate the Ansys model. When the situation of small flexures with a small rotation ( $\pm 5$  degrees) and a 90 Kg mass is considered (Figure 7.4) the differences between Ansys Workbench and Spacar are negligible. It is shown that the stress profiles and maximum stress are similar. The vibration modes of Ansys Workbench and Spacar are showed in Table 7.1 for the case of small flexures with the load of the mass of the mirrors. When the vibration modes are compared, it can be concluded that the frequencies have the same modes of deformation around the same values. Only the

third mode has a larger difference, but both these modes are far above the needed 30 Hz so the difference will not create an issue. Consequently, the Ansys Workbench model is validated and can be used to explore the option of tapered flexures.

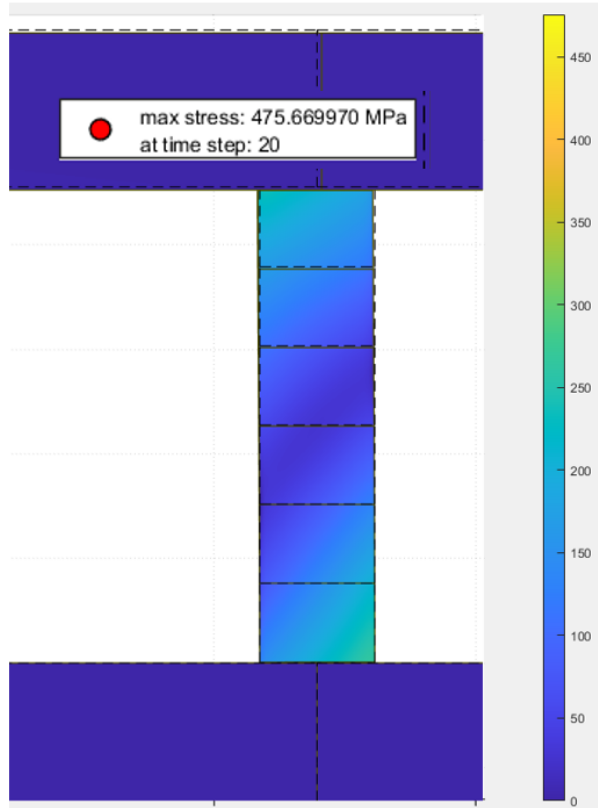
When a wider flexure or larger angles are used the difference between the software's becomes larger, Figure 7.5. This could be explained via the Wagner-torque effect. The Wagner-torque effect will increase quadratically when a torsion angle becomes large, especially in a system with wide flexures [15]. In Spacar the torsion angle and moment are linear dependents which is a good estimation for small flexures but not for large flexures. The difference in the application of this effect influences the stiffness of the flexures and resulting in a larger moment needed for the rotation, which is higher in Ansys Workbench, providing higher stresses in the flexures.

Table 7.1: Vibration modes Ansys Workbench and Spacar for the case of small flexures

Program	Mass	Vibration modes	Direction
Ansys Workbench	On	1. 1.86 Hz 2. 12.864 Hz 3. 12.866 Hz 4. 43.53 Hz	1. Rotation around z 2. Translation x 3. Translation y 4. Rotation around the mass
Spacar	On	1. 0.51 Hz 2. 15.42 Hz 3. 15.42 Hz 4. 58.58 Hz	1. Rotation around z 2. Translation x 3. Translation y 4. Rotation around the mass

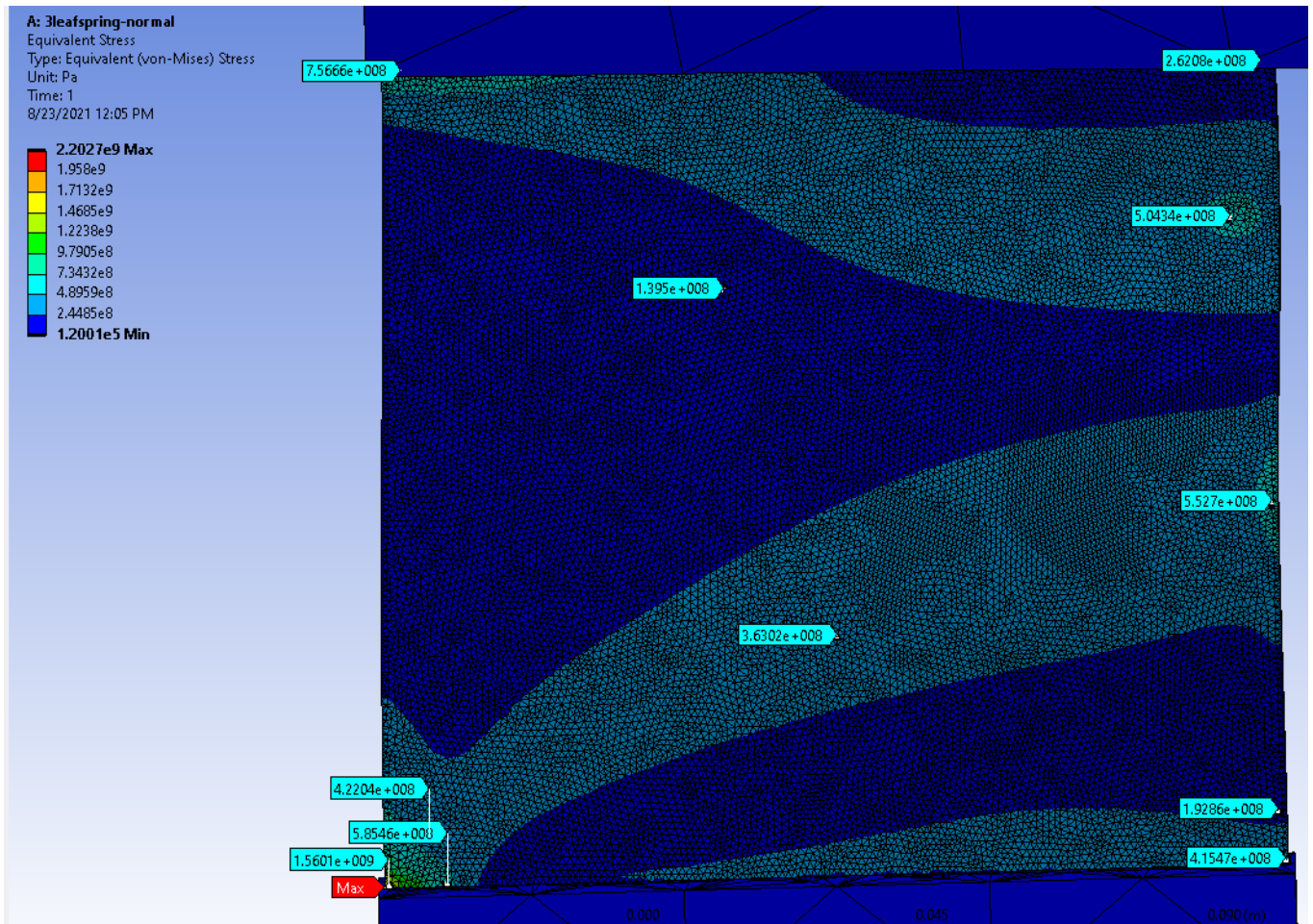


(a) Stress analysis of one flexure in Ansys Workbench

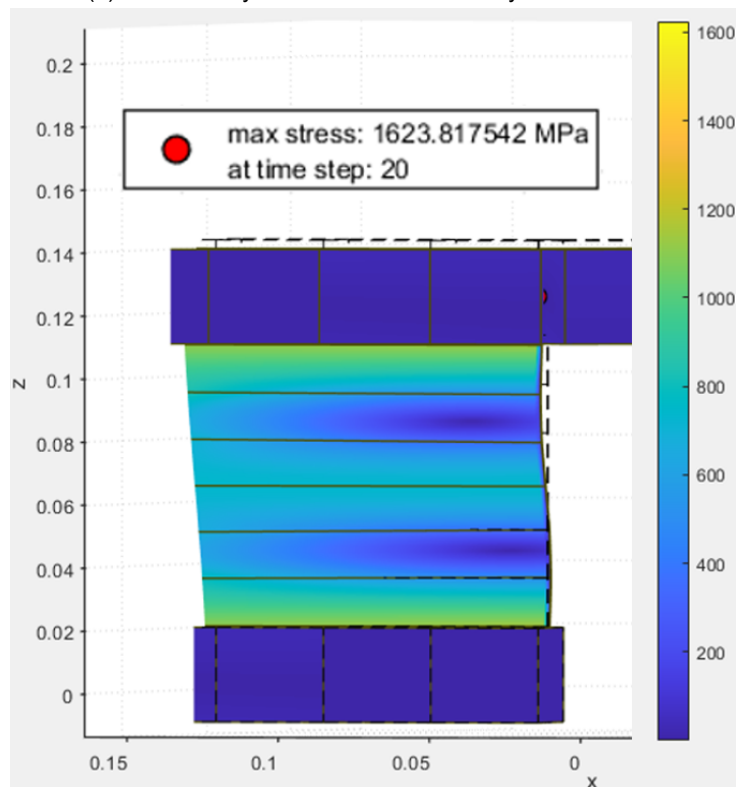


(b) Stress analysis of one flexure in Spacar

Figure 7.4: Comparison in stress analysis between Ansys Workbench and Spacar when a rotation of  $\pm 5$  degrees is applied



(a) Stress analysis of one flexure in Ansys Workbench



(b) Stress analysis of one flexure in Spacar

Figure 7.5: Comparison in stress analysis between Ansys Workbench and Spacar when wide flexures are used with a rotation of  $\pm 12$  degrees.

### 7.2.1 Tapered system

The tapered model, shown in Figure 7.7, has a tapering calculated with Equation 7.5. If this system is analysed in Ansys Workbench large stress points arise near the surfaces. This is the result of the connection used between the flexible and rigid part. According to the Saint Venant's principle, the stress on the surface can be altered by a different connection. Nevertheless, the stress in the middle parts remains the same [16]. For the comparisons between the tapering, the outer edges connected to the rigid part are neglected. If the two methods for tapering are compared, the conical shape provides the lowest stresses. The full comparison between the two methods and the stress analysis is shown in appendix F.1. For the case of a width of 50 mm and an angle of  $\pm 5$  degrees the stresses are shown in Figure 7.6. It can be concluded that the stress is lower than the maximum allowed stress and therefore results to a better performance. However, when a large angle is used the stress will increase rapidly and vibration modes reduce. A tapered 3-leaf spring with a width of 50 mm allows for a maximum angle of  $\pm 6$  degrees in order to keep the second vibration mode above 30 Hz.

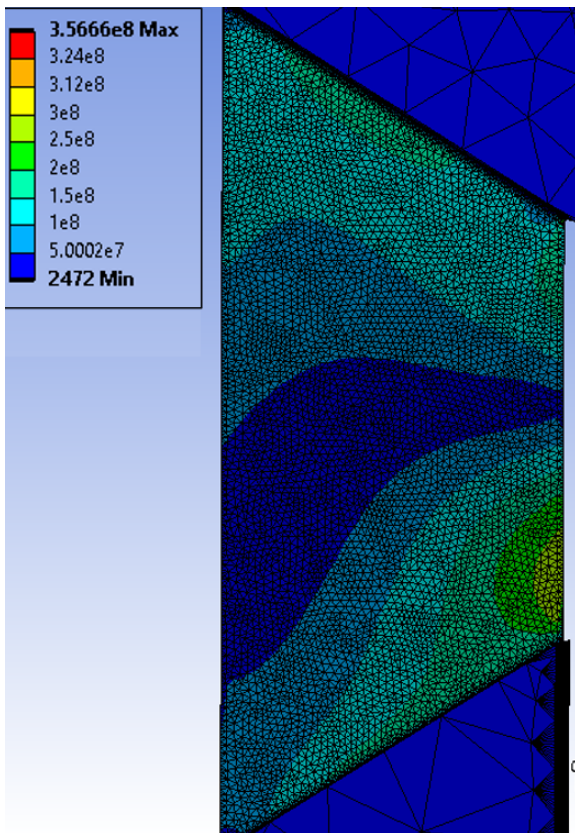


Figure 7.6: Stress analysis of the 3 leaf spring torsion concept with a conical tapering, a width of 50 mm and a rotation of 5 degrees

In the tapered model, the vibration modes are within a closer range of each other compared to the straight model. For the tapered model the first vibration mode, the desired motion, is 11.125 Hz and the second mode is 35.716 Hz which still is within the requirement.

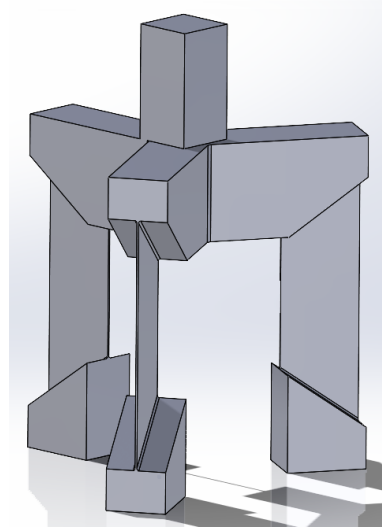


Figure 7.7: 3 leaf spring tapered

### 7.3 Final design

The 3 leaf spring torsion concept is not able to rotate the preferred rotation range with the current configuration. To double the allowable rotation it is possible to add the flexure system an extra time in series, Figure 7.8. By adding an extra level of flexure the stress will be divided between the two series of flexures, hence allowing a larger angle for the same amount of stress. When six flexures, 2 series of 3 parallel flexures, are used an angle of  $\pm 0.20$  rad ( $\pm 11$  degree) can be obtained with the same stress as a three flexures system.

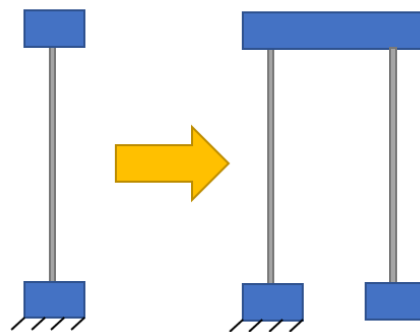


Figure 7.8: Schematic overview of the change for one flexure from a parallel to a series concept. The blue parts are rigid and the grey parts are the flexures

When the mass of the system is neglected the flexures in series divided the stress equally. Following, when the mass is included the stress on the first flexure is higher than the stress on the second flexure. The difference in stress is because the first flexure is being compressed, while the second flexure is stretched by the mass. There are two solutions for this problem; first different thicknesses for the flexures could be used. When the second flexure (stretched flexure) has a smaller thickness it will have higher stresses given all the flexures the same stress. However, this will lead to one weaker flexure (the one under tension) compared to the other flexure, creating stability problems in the system. The second solution is to use multiple points of actuation for rotation. Here both flexures are given the moment needed to perform the exact same deformation. The last approach is used in the final design.

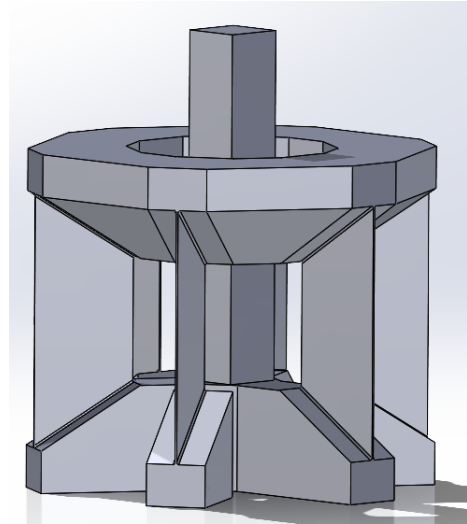


Figure 7.9: Final design 3 leaf spring torsion concept

Due to fatigue, the maximum angle reduces to  $\pm 3.5$  degrees per flexure, resulting in a total rotation of  $\pm 7$  degrees for the design with 2 flexures systems in series. With a further increase of levels of flexures it is expected that an even larger maximum rotation could be achieved, but this has not been analyzed further in the present study.

The properties of the final design are shown in Table 7.2. The second vibration mode appears to be too low (below the 30 Hz). However, the second mode is caused by the change to a series model and is also the desired rotation executed by the in-between body. How the vibration modes change during the rotation is not been investigated with Ansys workbench, so no accurate information is available. However, the third and fourth vibration modes are very large so no problem is foreseen.

The 3 leaf spring torsion concept has a simple and open structure which makes it possible to produce with milling, which is the main technique used by Astron Nova.

#### 7.4 Conclusion

With the addition of tapered instead of straight leafs the stress in the 3 leaf spring flexure can be reduced significantly. For the tapering, a conical shape provides the best stress distribution. When a life span of 18 year is considered the 3 leaf spring torsion concept series can rotate an angle of  $\pm 7$  degrees. The vibration modes throughout the rotation are not yet known. However, it is assumed that for the angle of  $\pm 3.5$  degrees per flexure there will be no problems. For the production of this concept the in house technique of Astron Nova can be used which is desired by the company.

Table 7.2: Properties 2 series 3 leaf spring torsion concept

Thickness	Angle	Stress incl. warping	Vibration modes incl. warping
0.9 mm	$\pm 0.1221 \text{ rad}$	149.85 MPa	1. 7.1943 Hz 2. 20.731 Hz 3. 104.62 Hz 4. 223.05 Hz

# 8 DISCUSSION, CONCLUSION AND RECOMMENDATIONS

## 8.1 Discussion and conclusion

This project was performed to find a solution for the design of a flexible hollow hinge in a cryogenic environment. The requirement for this system was to have a large angle of 22.5 degrees in both directions. This study shows that a flexure can be designed for the required motion in the cryogenic environment, but an angle of 22.5 degrees is not possible when the second and higher vibration modes need to be above 30 Hz. For most concepts, the second vibration mode decreases rapidly when the system is rotating. Thicker flexures could provide a solution for the vibration modes, nevertheless then the stress will become too high, resulting in the breakage of the flexure. To deal with the requirement for a maximum stress of 151 MPa, to prevent failure due to fatigue, the maximum angle of  $\pm 7$  degrees has been achieved.

Two found concepts allow a maximum rotation of  $\pm 7$  degrees; the 3 leaf spring torsion concept and the Butterfly. The Butterfly however only manages this angle when extra volume (20% more width and height) is added, while the 3 leaf spring torsion concept fits within the initial volume. Indicating that the 3 leaf spring torsion concept has a concession of one of the requirements, and the Butterfly has a concession on two requirements. Furthermore, the 3 leaf spring torsion concept is now designed in series with one extra layer of flexures. More layers will result in a larger angle, therefore, it is the best solution for the rotation of the mirrors in a cryogenic environment.

During the optimization of the concepts a correlation between stress and mass could be determined. The expectation that the stress of the flexure can be lowered by reducing the thickness, did not hold. Since, the mass of 90 Kg located above the flexures had a significant influence on the behaviour of the system. This resulted in a parabolic response of the stress when the thickness of the flexures was altered, which means the stress could be higher for thinner flexures compared to thicker flexures.

For the 3 leaf spring torsion model a study to the use of tapering has been performed. Based on this analysis, it can be concluded that tapering will provide a reduction in stress. Different widths are compared to find a balance between low stress and good vibration modes. Widths of 30, 50 and 70 mm are investigated. The results show that the second and third vibration modes for 30 mm are too low, but at 50 mm they met the required value. The range between 30 and 50 mm is not further investigated to find width and thickness that satisfies the vibration modes, and have lower stress than the 50 mm model. In addition, the change in the second vibration mode, due to the rotation movement is not researched. This could have some impact on the maximum angle, therefore further research could be performed to analyse these optimisations.

Hopkins discusses in his paper on FACT [8] that when 5 non-redundant constraint lines are chosen his theory will lead to the exact DoFs. However, in the optimisation of the concepts, some concepts showed vibration modes indicating a system with more than one DoF. Therefore, it can be concluded that for a small volume the distance between the constraint lines is too small to be non-redundant. In order to have the right number of DoFs more distance between the constraint lines and/or extra flexures need to be added. This can be seen from the difference in vibration modes and explains why some concepts benefit from a larger volume. The larger the distance between the constraint lines the stiffer the system is. Resulting in a significant difference between the vibration modes.

For the optimizations of the concepts the multi-body software Spacar is used. Chapter 7 shows that small flexures rotating under a small angle provides matching results with FEM software. However, when larger rotations and/or flexures are used the results differ. This is explained via the absence of effects in Spacar, like the Wagner-torque effect. It is assumed that the impact of this effect is the largest for the 3 leaf spring torsion

concepts, because of the width of the flexure. However, there might be some effects for other concepts as well.

During this project the material AL 6061T6 is used, because it has well-known properties in a cryogenic environment. However, throughout the optimizations, the maximum allowed stress had an impact on the size of the rotations, especially when fatigue is considered. An search into different materials with higher stress levels was not performed, because it was beyond the scope of this research.

In the simulations in Spacar, the shape of the rigid bodies is determined by the software. The collision of objects is not included in Spacar, therefore the rigid parts are drawn in a direct line to each other. In addition, during the simulations the center of the flexures have rigid parts connecting to the center of mass. However, this is not possible in the final design. A redesign considering the connection to the mirrors needs to be performed. When the rigid bodies are redesigned to fit in the available space, the change in shape can influence the vibration modes. This should be taken into account when a design is developed further.

In conclusion, it is possible to use a flexible hinge in a cryogenic environment for the rotation of the 3-mirror system of METIS with a maximum stress of 151 MPa and vibration modes above the 30 Hz. However, the rotation will not be the desired 22.5 degrees, but a rotation of  $\pm 7$  degrees, resulting in a total rotation of 14 degrees within the given volume. However, this can potentially be increased by adopting the recommended modifications.

## 8.2 Recommendations

Before the 3 leaf spring torsion concept can be placed in METIS more research needs to be performed on different aspects of the model.

Firstly, a more in-depth study of the width of the flexures needs to be performed. In this research, a width of 50 mm is taken as the best solution, but no research is done on the stress and vibration modes for flexures between the 30 and 50 mm. Possibly 40 mm will be a optimal compromise of the high vibration modes of the 50 mm model and the low stress of the 30 mm model. In addition, the influence of the thickness on the different widths should be taken into account as well.

Secondly, in this study the change in vibration modes of the 3 leaf spring torsion concept when the system is rotating is not determined with Ansys Workbench. The Spacar model shows that the second vibration mode will probably decrease as a result of the movement, but the impact of the decrease is not studied. More research will be needed to determine if the second vibration mode for a  $\pm 7$  degree angle remains above the 30 Hz throughout the rotation.

Thirdly, for the final design of the 3 leaf spring torsion concept a series of 2 layers of flexures is used. Nevertheless, there is still space available in the initial volume to add an extra layer of flexures. This could result in a larger angle, while keeping the same stress values. However, the influence of an extra layer of flexures on the vibration modes need to be investigated.

Lastly, after the first concept reduction (Chapter 4.3) it was chosen to only work out the 3 leaf spring torsion concept and to leave the 4 leaf spring torsion concept. This was chosen because the stress of the 4 leaf spring torsion concept was higher compared to the 3 leaf spring torsion concept. However, the 4 leaf spring torsion concept had higher vibration modes indicated to be a stiffer system. A study into the benefits of adding an extra flexure to the system needs to be done. This might lead to a model with smaller flexure, because of the stiffness and/or thinner flexures because the mass will be distributed over more flexures.

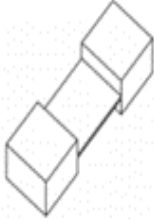
# REFERENCES

- [1] Nicolae Lobontiu. *Compliant Mechanisms: Design of Flexure Hinges*. 12 2002.
- [2] Hun Byoung, John Kang, Yung Ting, J.T. Wen, Jason Dagalakis, and Gorman. Analysis and design of parallel mechanisms with flexure joints. *IEEE transactions on robotics*, 21, 01 2005.
- [3] S. Henein, P. Spanoudakis, S. Droz, I. Myklebust, E. Onillon, and Suisse d'Electronique. Flexure pivot for aerospace mechanisms. 2007.
- [4] J.E. Speich M. Goldfarb. A well-behaved revolute flexure joint for compliant mechanism design. *Journal of Mechanical Design*, 121, 09 199.
- [5] Nicola Bailey, Christopher Lusty, and Patrick Keogh. Nonlinear flexure coupling elements for precision control of multibody systems. *Proceedings of the Royal Society A: Mathematical, Physical and Engineering Sciences*, 474, 2018.
- [6] ESO. The european extremely large telescope (elt) project. 2019.
- [7] Nova. Graduation project assignment nova astron. 2020.
- [8] Jonathan Hopkins. Design of parallel flexure systems via freedom and constraint topologies (fact). 2008.
- [9] James Clerk Maxwell and W. D. Niven. *The Scientific Papers of James Clerk Maxwell*. Dover Press, 1876.
- [10] D.L. Blanding. *Exact Constraint: Machine Design Using Kinematic Principles*. ASME Press, New York, 1999.
- [11] Jurnan Schilder and Ronald Aarts. Flexible multibody dynamics. 2021.
- [12] Olivier A. Bauchau. *Flexible Multibody Dynamics*. Springer Netherlands, 2011.
- [13] D.M. Brouwer, J.P. Meijaard, and J.B. Jonker. Large deflection stiffness analysis of parallel prismatic leaf-spring flexures. *Precision Engineering*, 37(3):505–521, 2013.
- [14] Layton Hale. Principles and techniques for designing precision machines. 1999.
- [15] Willem Jan Raven. Nieuwe blik op knip en knik. 2006.
- [16] R. A. Toupin. On st. venant's principle. pages 151–152, 1966.
- [17] Jianwei Wu, Shuai Cai, Jiwen Cui, and Jiubin Tan. A generalized analytical compliance model for cartwheel flexure hinges. *Review of Scientific Instruments*, 86:105003, 10 2015.
- [18] Yakov Tseytlin. Notch flexure hinges: An effective theory. *Review of Scientific Instruments*, pages 3363 – 3368, 10 2002.
- [19] Ronald Aarts, D. Wiersma, Steven Boer, and Dannis Brouwer. Design and performance optimization of large stroke spatial flexures. *Journal of Computational and Nonlinear Dynamics*, 9:011016–011025, 10 2013.
- [20] Xu Pei, Jingjun Yu, Guanghua Zong, Shusheng Bi, and Hai-Jun Su. The modeling of cartwheel flexural hinges. *Mechanism and Machine Theory*, 44:1900–1909, 10 2009.
- [21] Mark Naves, R.G.K.M. Aarts, and Dannis Michel Brouwer. Large-stroke flexure hinges: Building-block-based spatial topology synthesis method for maximising flexure performance over their entire range of motion. *Mikroniek*, 57(3):5–9, 2017.
- [22] Simon Henein, Peter Spanoudakis, Serge Droz, Leif Myklebust, and Emmanuel Onillon. Flexure pivot for aerospace mechanisms. *European Space Agency, (Special Publication) ESA SP*, 01 2003.
- [23] Mentor Dynamics. Powerpack spiral spring; double torsion, 2018.

# A EXISTING FLEXURES

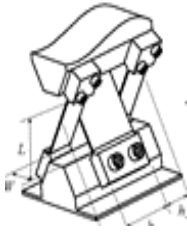
In this appendix, the results of the study into existing and commonly used rotational flexures is given. The advantages and the disadvantages as experienced in practice are mentioned for each flexure.

Table A.1: Common rotational flexures

Name	Image	Advantages	Disadvantages
Notch hinge	 <p>[17]</p>	<ul style="list-style-type: none"> <li>• High off-axis stiffness [17]</li> <li>• High rotational precision [17]</li> <li>• Easy to manufacture</li> <li>• Stable kinematics [18]</li> <li>• Small dimensions [18]</li> </ul>	<ul style="list-style-type: none"> <li>• Stress concentration results in localization of strains which gives a limited range of motion [17]</li> <li>• Complex stress conditions [18]</li> </ul>
Leaf spring	 <p>[17]</p>	<ul style="list-style-type: none"> <li>• Higher deflection than a notch hinge [17]</li> <li>• Simply constructed</li> </ul>	<ul style="list-style-type: none"> <li>• Difficult to obtain high precision for large range of motion because of the parasitic error [17]</li> <li>• Rotation point not localized [18]</li> <li>• Low stiffness in rotation around z direction [17]</li> </ul>
Flexure Cross hinge	 <p>[17]</p>	<ul style="list-style-type: none"> <li>• Improved precision without decreasing the range of motion [17]</li> <li>• The stress is not concentrated in 1 point, so the flexure can be shorter [19]</li> <li>• Pivots at the intersection point [19]</li> <li>• Symmetric geometry</li> </ul>	<ul style="list-style-type: none"> <li>• Constrained warping needs to be included (increase of torsional stiffness) [19]</li> <li>• Non-ideal kinematic behaviour [4]</li> </ul>

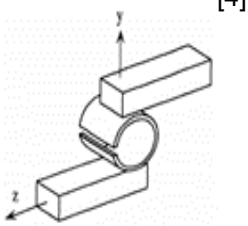
Continued on next page

Table A.1 – Continued from previous page

Name	Image	Advantages	Disadvantages
Three flexure Cross hinge	 <p>[19]</p>	<ul style="list-style-type: none"> <li>• Improved precision without decreasing the range of motion [17]</li> <li>• The stress is not concentrated in 1 point, so the flexure can be shorter [19]</li> <li>• Symmetric geometry</li> <li>• Pivots at the intersection point [19]</li> </ul>	<ul style="list-style-type: none"> <li>• Constrained warping needs to be included (increase of torsional stiffness [19])</li> <li>• Low rotational precision [20]</li> <li>• Needs to be assembled [20]</li> <li>• Non-ideal kinematic behaviour [4]</li> </ul>
Curved flexure hinge	 <p>[19]</p>	<ul style="list-style-type: none"> <li>• The stiffness is distributed over the range of motion</li> <li>• Symmetric geometry</li> <li>• Pivots at the intersection point [19]</li> </ul>	<ul style="list-style-type: none"> <li>• Initially gives 2 DoF [19] (the rotation about the z-axis and the translation in x-direction)</li> <li>• Will quickly reduce to a three flexure cross hinge [19]</li> <li>• Needs to be assembled [20]</li> <li>• Non-ideal kinematic behaviour [4]</li> </ul>
Cartwheel hinge	 <p>[17]</p>	<ul style="list-style-type: none"> <li>• High precision [17]</li> <li>• Large deflections [17]</li> <li>• High rotational precision [20]</li> <li>• Symmetric geometry</li> </ul>	<ul style="list-style-type: none"> <li>• Stress concentrated in 1 point [19]</li> <li>• Non-ideal kinematic behaviour [4]</li> </ul>
T-flexure	 <p>[21]</p>	<ul style="list-style-type: none"> <li>• Large range of motion</li> <li>• High stiffness [21]</li> <li>• Optimized to maximize parasitic frequency [21]</li> </ul>	<ul style="list-style-type: none"> <li>• Complex design</li> <li>• Difficult to make hollow</li> </ul>
Butterfly pivot	 <p>[22]</p>	<ul style="list-style-type: none"> <li>• Almost non center shift [22]</li> <li>• Good for vibrations [22]</li> <li>• High stiffness [22]</li> <li>• Symmetric geometry</li> </ul>	<ul style="list-style-type: none"> <li>• Range of motion between 7,5 and 10 degree [22]</li> <li>• 8 flexures are needed for one hinge</li> <li>• Complex design</li> </ul>

Continued on next page

**Table A.1 – Continued from previous page**

Name	Image	Advantages	Disadvantages
Split tube		<ul style="list-style-type: none"> <li>• Large range of motion</li> <li>• High precision [4]</li> <li>• Single axis of rotation [4]</li> </ul>	<ul style="list-style-type: none"> <li>• Doesn't work as well in practice</li> <li>• Low stiffness in y- direction [4]</li> </ul>
Double spiral torsion spring		<ul style="list-style-type: none"> <li>• Large range of motion</li> <li>• Low stiffness [23]</li> </ul>	<ul style="list-style-type: none"> <li>• Very flexible in all the directions, so should be housed in [23]</li> <li>• Reacts more like a spring than a flexure</li> </ul>

# B FACT

With Maxwell's contribution and Baldings's rule, explained in the main text, Hopkins has come up with an overview of all possible design situations and there corresponding constraint lines/planes.

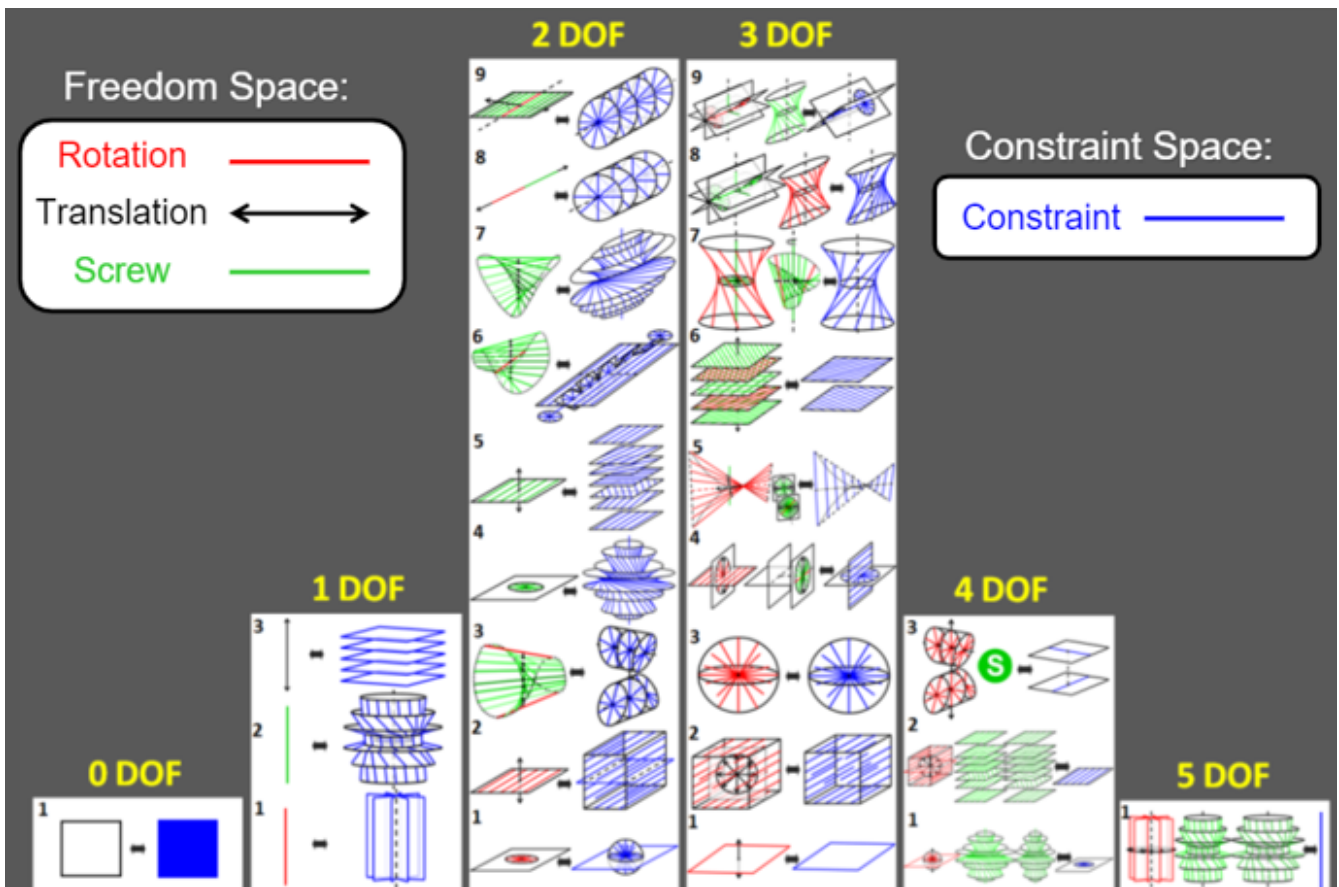
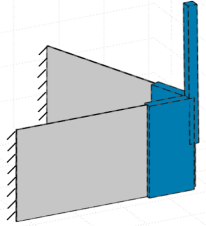
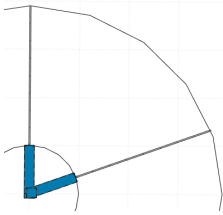
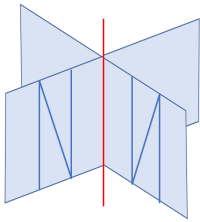
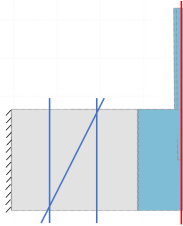
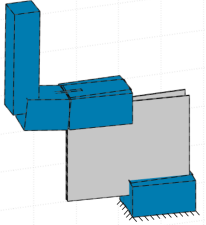
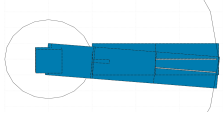
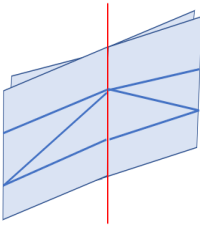
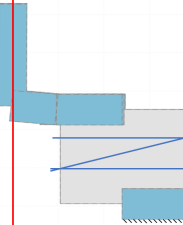


Figure B.1: Complete FACT Library for Parallel Systems [8]

# C LIST OF CONCEPTS

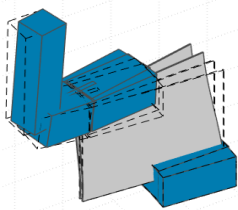
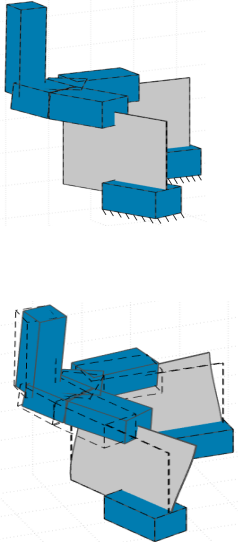
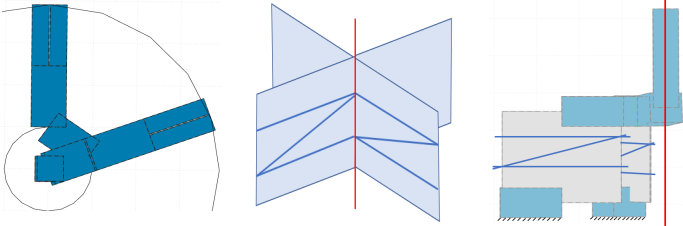
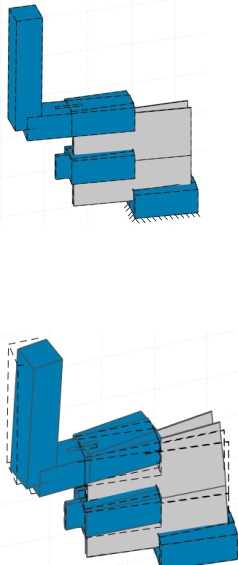
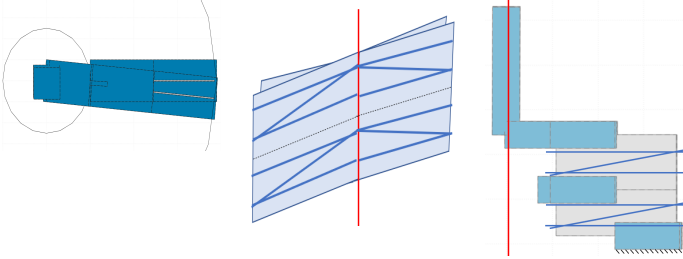
Multiple concepts have been developed during this study. The concepts are inspired by existing flexures and/or the FACT method. An overview of all the concepts investigated during this project are discussed below. In the figures, the blue parts are rigid, while the grey parts are the flexures. When lines are used the blue line represents the constraint line and the red the freedom line. In the top views a circle is visible indicating the available volume for the flexures.

Table C.1: Concepts

Concepts				
<p><b>2 leaf spring</b></p> <p>Tilted (3D) view Top view - Constraint lines - Side view</p> <p>Max deflection</p>				 <p>2 leaf springs connected to the fixed world at the side edges of the leaf springs. The system has one overconstraint.</p>
<p><b>2 leaf spring torsion</b></p> <p>Tilted (3D) view Top view - Constraint lines - Side view</p>				

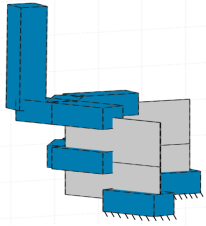
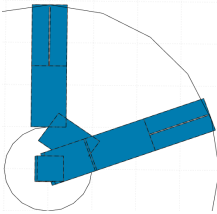
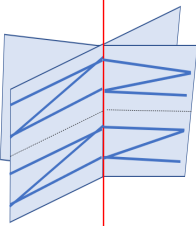
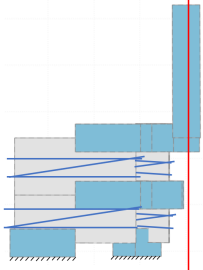
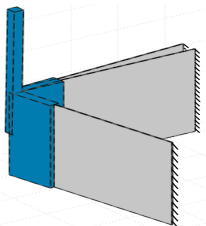
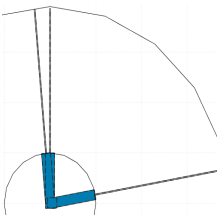
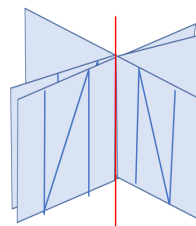
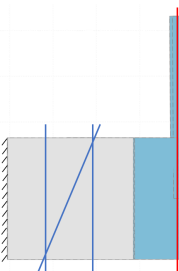
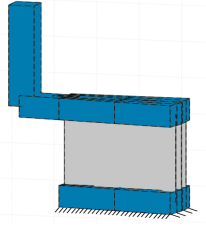
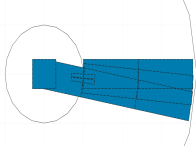
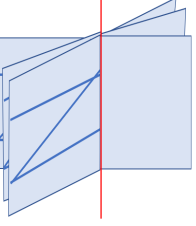
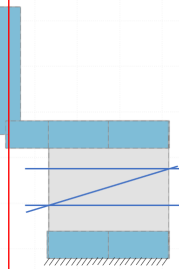
Continued on next page

Table C.1 – Continued from previous page

Concepts		
<p>Max deflection</p>		<p>2 leaf springs under an angle of 5 degrees. The bottom part of the flexures is connected to the fixed world, while the tops are connected together. The system has 1 overconstraint.</p>
<p><b>2 leaf spring torsion large</b></p> <p>Tilted (3D) view Top view - Constraint lines - Side view</p> <p>Max deflection</p>		 <p>2 leaf springs under an angle of 70 degrees. The bottom part of the flexures is connected to the fixed world, while the tops are connected together. The system has 1 overconstraint.</p>
<p><b>2 leaf spring torsion double small</b></p> <p>Tilted (3D) view Top view - Constraint lines - Side view</p> <p>Max deflection</p>		 <p>4 leaf springs where two leaf springs are stacked on top of each other. The two stacks are placed under an angle of 5 degrees. The bottom part of the flexures is connected to the fixed world, while the tops are connected. The system has 7 overconstraints.</p>

Continued on next page

Table C.1 – Continued from previous page

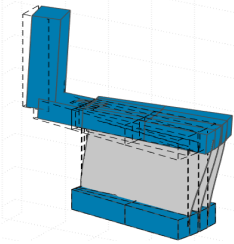
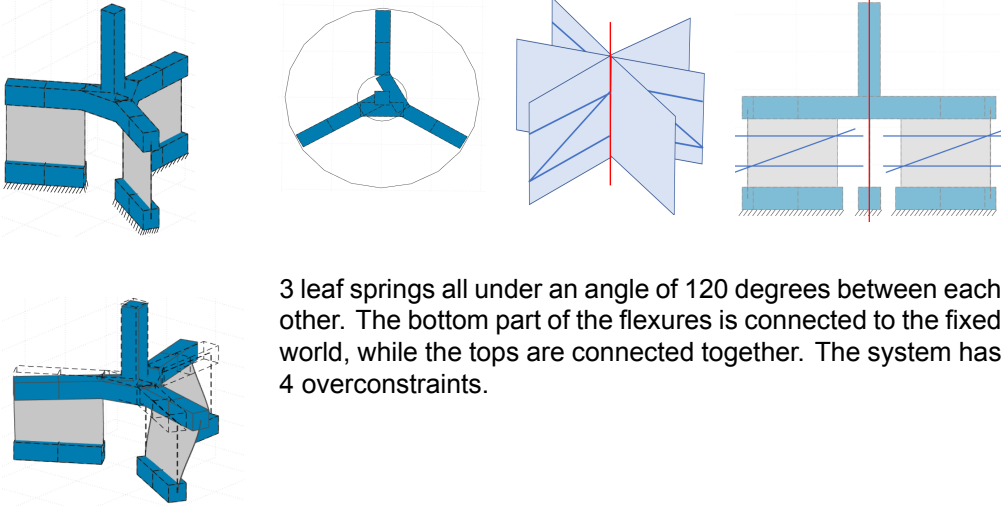
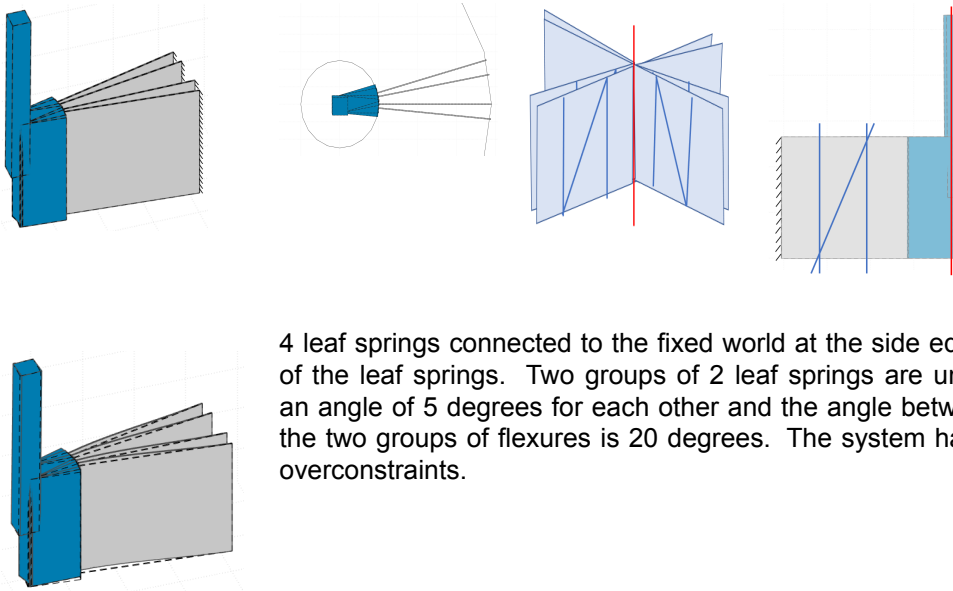
Concepts				
<p><b>2 leaf spring torsion double</b></p> <p>Tilted (3D) view Top view - Constraint lines - Side view</p> <p>Max deflection</p>				
<p><b>3 leaf springs</b></p> <p>Tilted (3D) view Top view - Constraint lines - Side view</p> <p>Max deflection</p>				
<p><b>3 leaf spring torsion small</b></p> <p>Tilted (3D) view Top view - Constraint lines - Side view</p>				

4 leaf springs where 2 leaf springs are stacked on top of each other. The 2 stacks are placed under an angle of 70 degrees. The bottom part of the flexures is connected to the fixed world, while the tops are connected. The system has 7 overconstraints.

3 leaf springs connected to the fixed world at the side edges of the leaf springs. 2 leaf springs are under an angle of 5 degrees from each other and the last flexure is under an angle of 30 degree from the other two. The system has 4 overconstraints.

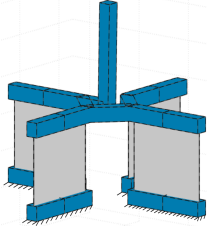
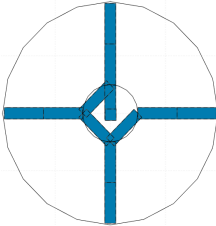
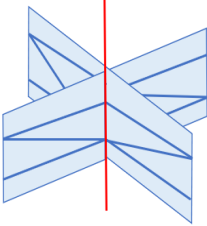
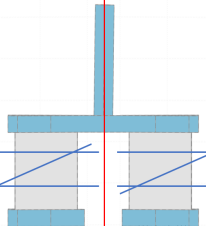
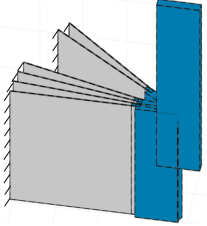
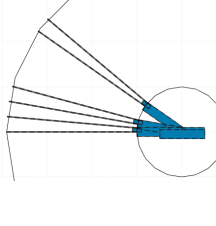
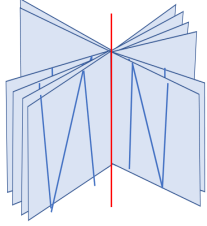
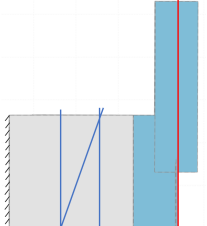
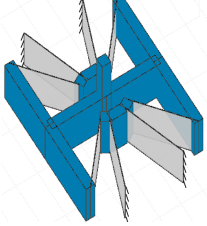
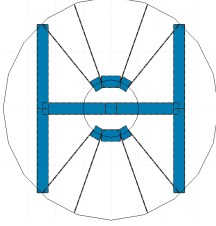
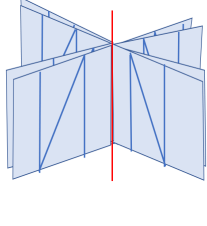
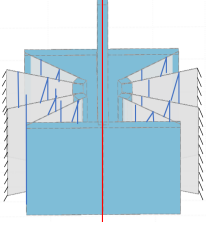
Continued on next page

Table C.1 – Continued from previous page

Concepts		
<p>Max deflection</p>		<p>3 leaf springs all under an angle of 5 degrees for each other. The bottom part of the flexures is connected to the fixed world, while the tops are connected together. The system has 4 overconstraints.</p>
<p><b>3 leaf spring torsion</b></p> <p>Tilted (3D) view Top view - Constraint lines - Side view</p> <p>Max deflection</p>		<p>3 leaf springs all under an angle of 120 degrees between each other. The bottom part of the flexures is connected to the fixed world, while the tops are connected together. The system has 4 overconstraints.</p>
<p><b>4 leaf springs</b></p> <p>Tilted (3D) view Top view - Constraint lines - Side view</p> <p>Max deflection</p>		<p>4 leaf springs connected to the fixed world at the side edges of the leaf springs. Two groups of 2 leaf springs are under an angle of 5 degrees for each other and the angle between the two groups of flexures is 20 degrees. The system has 7 overconstraints.</p>

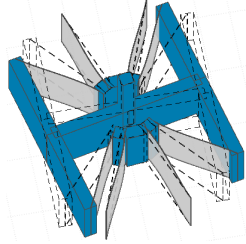
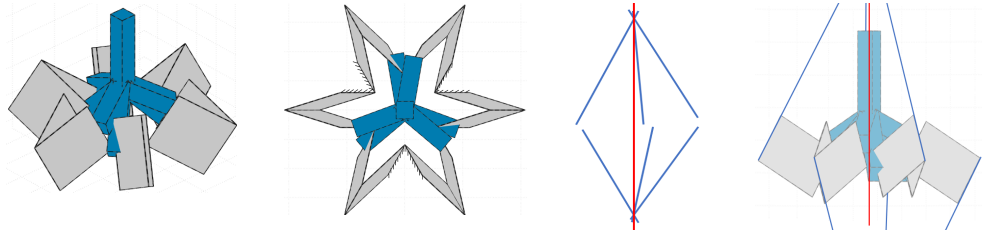
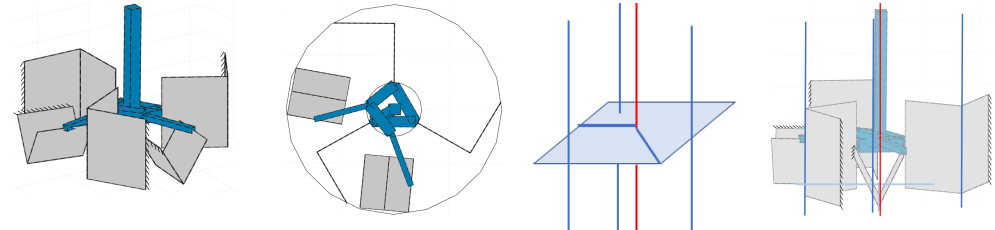
Continued on next page

Table C.1 – Continued from previous page

Concepts				
<p><b>4 leaf spring torsion</b></p> <p>Tilted (3D) view Top view - Constraint lines - Side view</p> <p>Max deflection</p>				 <p>4 leaf springs all under an angle of 90 degrees for each other. The bottom part of the flexures is connected to the fixed world, while the tops are connected together. The system has 7 overconstraints.</p>
<p><b>6 leaf springs</b></p> <p>Tilted (3D) view Top view - Constraint lines - Side view</p> <p>Max deflection</p>				 <p>6 leaf springs connected to the fixed world at the side edges of the leaf springs. 2 leafs springs are located 30 degrees further than the other 4. This is done to get a more stable system. The other 4 flexures are under an angle of 5 degrees for each other to keep the stress low. The system has 13 overconstraints.</p>
<p><b>Butterfly</b></p> <p>Tilted (3D) view Top view - Constraint lines - Side view</p>				

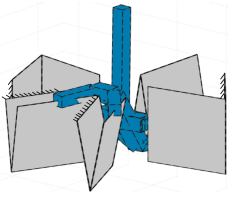
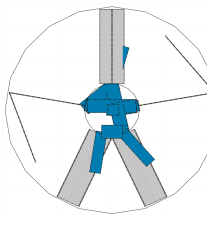
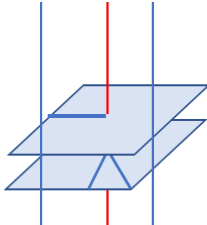
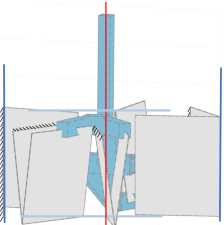
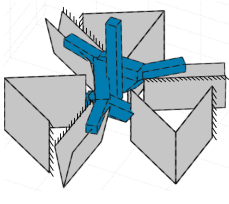
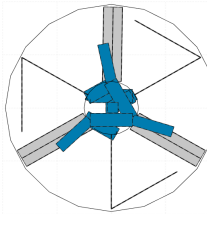
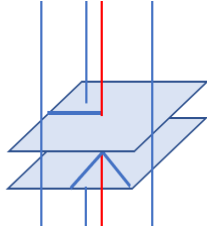
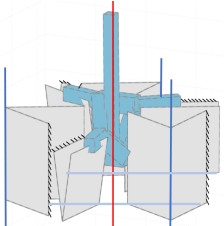
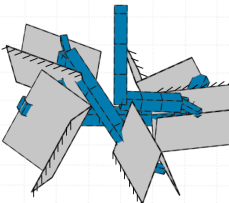
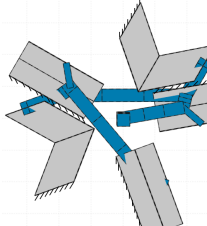
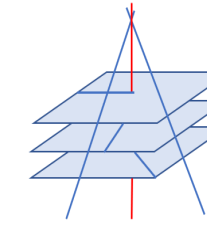
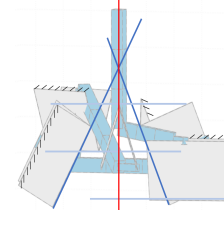
Continued on next page

**Table C.1 – Continued from previous page**

Concepts				
<p>Max deflection</p>	 <p>This concept consists of 8 leaf springs connected in series. The middle 4 leaf springs are on one side connected to the fixed world and the other side connected to a middle body. The middle bodies are then both connected by 2 leaf springs to the H framed body. The system has 3 overconstraints.</p>			
<p><b>Concept 1</b></p> <p>Tilted (3D) view Top view - Constraint lines - Side view</p> <p>Max deflection</p>	 <p>The system consisted of 6 folded leaf springs. 3 folded leaf springs are located at the top and are angled to a point on the rotation line above the used volume. The other three are placed at the bottom of the volume and angled to a point on the rotation axis below the volume. The distance between the two points gives the system only one degree of freedom. The system has 1 overconstraint.</p>			
<p><b>Concept 2</b></p> <p>Tilted (3D) view Top view - Constraint lines - Side view</p> <p>Max deflection</p>	 <p>5 folded leaf springs where 2 are horizontal in the same plane, but under different angles and 3 are vertical under an angle of 120 degrees from each other. The system has no overconstraints.</p>			

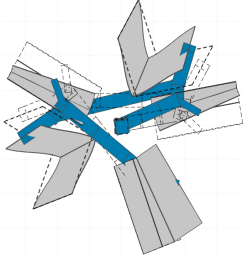
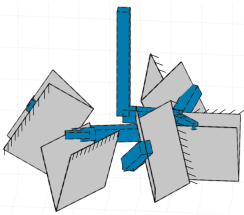
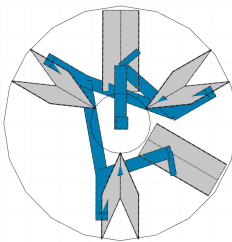
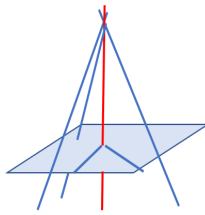
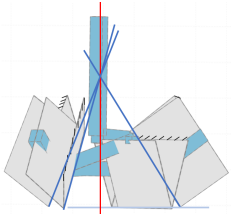
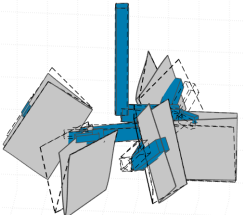
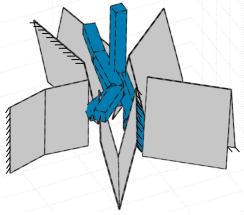
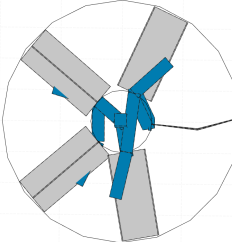
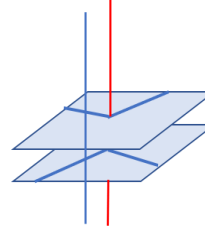
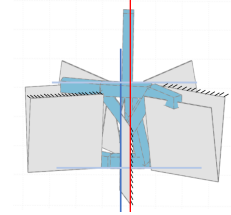
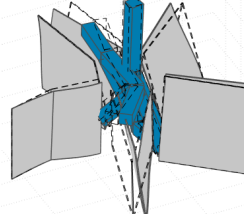
Continued on next page

Table C.1 – Continued from previous page

Concepts				
<p><b>Concept 2.2</b></p> <p>Tilted (3D) view Top view - Constraint lines - Side view</p> <p>Max deflection</p>				 <p>5 folded leaf springs where 3 are horizontal at 2 different heights under an angle of 120 degrees and 2 are vertical. The system has no overconstraints.</p>
<p><b>Concept 2.3</b></p> <p>Tilted (3D) view Top view - Constraint lines - Side view</p> <p>Max deflection</p>				 <p>6 folded leaf springs where three are horizontal divided over 2 planes at different heights under an angle of 120 degrees and 3 are vertical also under a 120 degrees angle. The system has 1 overconstraint.</p>
<p><b>Concept 3</b></p> <p>Tilted (3D) view Top view - Constraint lines - Side view</p>				

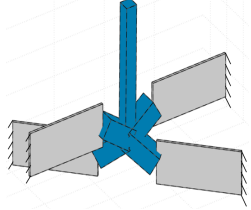
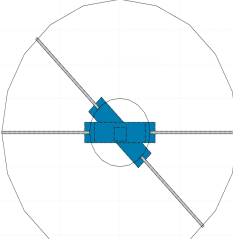
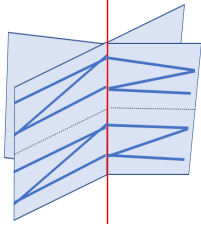
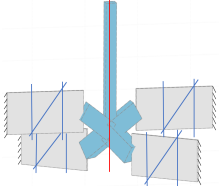
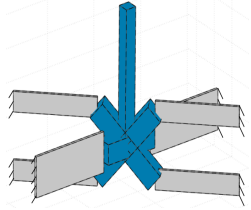
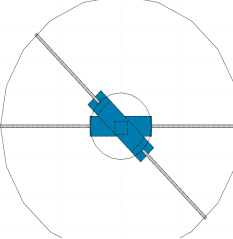
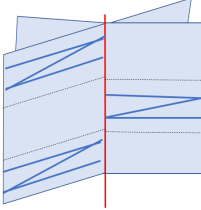
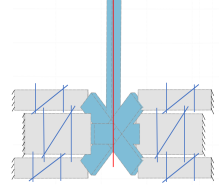
Continued on next page

**Table C.1 – Continued from previous page**

Concepts				
<p>Max deflection</p>	 <p>The system has 5 folded leaf springs, 2 are angled so the constraint lines intersect at a point on the rotation axis. 3 are horizontal where 2 are in the same plane under different angles and the last one is placed higher. This system has no overconstraints.</p>			
<p><b>Concept 3.2</b></p> <p>Tilted (3D) view Top view - Constraint lines - Side view</p> <p>Max deflection</p>				
<p>Max deflection</p>	 <p>The system has 5 folded leaf springs, 3 are angled so the constraint lines intersect at a point on the middle axis, which will become the rotation axis. The other 2 are horizontal in the same plane under different angles. This system has no overconstraints.</p>			
<p><b>Concept 4</b></p> <p>Tilted (3D) view Top view - Constraint lines - Side view</p> <p>Max deflection</p>				
<p>Max deflection</p>	 <p>5 folded leaf springs, where 4 are horizontal. The 4 horizontal constraint lines are divided into 2 horizontal constraint lines per plane. All the lines are under different angles to make sure the lines are non-redundant. The last constraint line is vertical in z-direction. The system has no overconstraints.</p>			

Continued on next page

Table C.1 – Continued from previous page

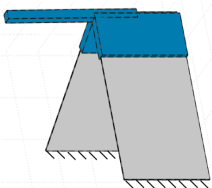
Concepts				
<p><b>Concept 7</b></p> <p>Tilted (3D) view Top view - Constraint lines - Side view</p> <p>Max deflection</p>				 <p>This system is based on the well-known cartwheel. It consists of 4 leaf springs where 2 are elongated form of each other. The system has 7 overconstraints.</p>
<p><b>Concept 8</b></p> <p>Tilted (3D) view Top view - Constraint lines - Side view</p> <p>Max deflection</p>				 <p>This system consists of 6 leaf springs where they are grouped where 2 are in each other's elongation. The system has 13 overconstraints.</p>

## D CONCEPT OPTIMIZATION

### D.1 Results of the optimization of the concepts

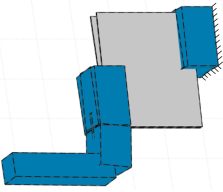
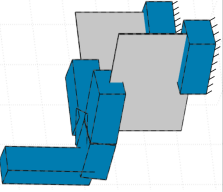
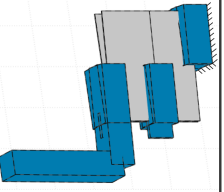
In this Appendix, the results of the optimization of the concepts are shown. The stress for an angle of  $\pm 0.22$  rad with and without the influence of warping are listed, where the stress of the model with warping is a better representation of the "real" world than the stress of the model without warping. Therefore, only the vibration modes of the model with warping are included. Finally the off centering of the mid point of the concepts are shown. For this three vectors are used, x, y and z, where a pure movement is one in the z-direction and zero in x- and y-direction.

Table D.1: Results of the concept analysis

Concept	Figure	Thickness	Stress excl. warping	Stress incl. warping	Vibration modes incl. warping	Off centering
2 leaf spring		1.3 mm	434.86 MPa	741.40 MPa	1. 1.52 Hz 2. 24.37 Hz 3. 31.64 Hz	<ul style="list-style-type: none"> <li>• x: -0.0951</li> <li>• y: -0.1686</li> <li>• z: 0.9811</li> </ul>

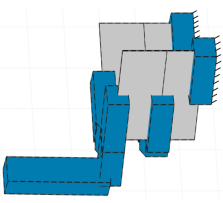
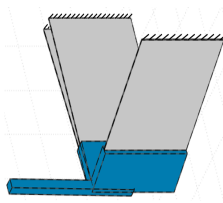
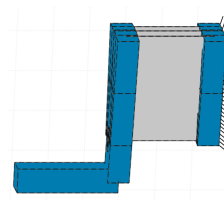
Continued on next page

Table D.1 – Continued from previous page

Concept	Figure	Thickness	Stress excl. warping	Stress incl. warping	Vibration modes incl. warping	Off centering
<b>2 leaf spring torsion small</b>		1.3 mm	380.08 MPa	741.40 MPa	<ol style="list-style-type: none"> <li>1. 2.19 Hz</li> <li>2. 4.09 Hz</li> <li>3. 9.95 Hz</li> </ol>	<ul style="list-style-type: none"> <li>• x: 0.0681</li> <li>• y: -0.0285</li> <li>• z: 0.9973</li> </ul>
<b>2 leaf spring torsion</b>		1.2 mm	525.69 MPa	1160.48 MPa	<ol style="list-style-type: none"> <li>1. 2.16 Hz</li> <li>2. 27.11 Hz</li> <li>3. 50.41 Hz</li> </ol>	<ul style="list-style-type: none"> <li>• x: 0.0198</li> <li>• y: 0.0277</li> <li>• z: 0.9994</li> </ul>
<b>2 leaf spring torsion double small</b>		0.9 mm	844.98 MPa	1711.81 MPa	<ol style="list-style-type: none"> <li>1. 2.28 Hz</li> <li>2. 3.66 Hz</li> <li>3. 9.23 Hz</li> </ol>	<ul style="list-style-type: none"> <li>• x: 0.0393</li> <li>• y: -0.1353</li> <li>• z: 0.9900</li> </ul>

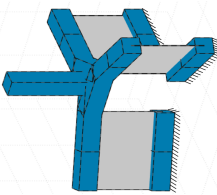
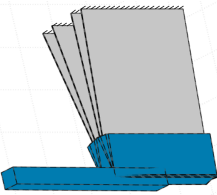
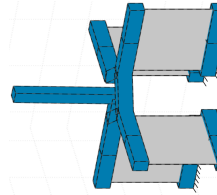
Continued on next page

Table D.1 – Continued from previous page

Concept	Figure	Thickness	Stress excl. warping	Stress incl. warping	Vibration modes incl. warping	Off centering
<b>2 leaf spring torsion double</b>		1.1 mm	1145.92 MPa	2367.10 MPa	<ol style="list-style-type: none"> <li>1. 3.58 Hz</li> <li>2. 24.89 Hz</li> <li>3. 49.97 Hz</li> </ol>	<ul style="list-style-type: none"> <li>• x: 0.0039</li> <li>• y: 0.0043</li> <li>• z: 1.0000</li> </ul>
<b>3 leaf spring</b>		1.1 mm	395.17 MPa	656.90 MPa	<ol style="list-style-type: none"> <li>1. 1.47 Hz</li> <li>2. 24.75 Hz</li> <li>3. 40.01 Hz</li> </ol>	<ul style="list-style-type: none"> <li>• x: -0.1088</li> <li>• y: -0.1641</li> <li>• z: 0.9804</li> </ul>
<b>3 leaf spring torsion small</b>		1.1 mm	366.37 MPa	902.09 MPa	<ol style="list-style-type: none"> <li>1. 2.23 Hz</li> <li>2. 7.28 Hz</li> <li>3. 17.47 Hz</li> </ol>	<ul style="list-style-type: none"> <li>• x: 0.0141</li> <li>• y: 0.0234</li> <li>• z: 0.9996</li> </ul>

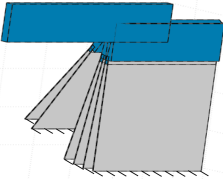
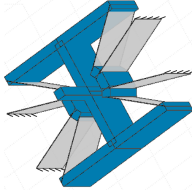
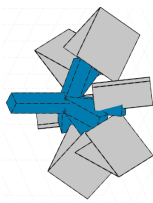
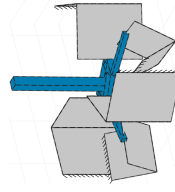
Continued on next page

Table D.1 – Continued from previous page

Concept	Figure	Thickness	Stress excl. warping	Stress incl. warping	Vibration modes incl. warping	Off centering
<b>3 leaf spring torsion</b>		0.8e mm	324.47 MPa	1886.39 MPa	<ol style="list-style-type: none"> <li>1. 0.55 Hz</li> <li>2. 61.23 Hz</li> <li>3. 62.29 Hz</li> </ol>	<ul style="list-style-type: none"> <li>• x: 0.0007</li> <li>• y: 0.0002</li> <li>• z: 1.0000</li> </ul>
<b>4 leaf springs</b>		1.1 mm	530.40 MPa	901.95 MPa	<ol style="list-style-type: none"> <li>1. 1.68 Hz</li> <li>2. 9.66 Hz</li> <li>3. 37.73 Hz</li> </ol>	<ul style="list-style-type: none"> <li>• x: 0.4161</li> <li>• y: -0.1626</li> <li>• z: 0.8947</li> </ul>
<b>4 leaf spring torsion</b>		0.7 mm	405.59 MPa	2083.57 MPa	<ol style="list-style-type: none"> <li>1. 0.42 Hz</li> <li>2. 84.74 Hz</li> <li>3. 104.30 Hz</li> </ol>	<ul style="list-style-type: none"> <li>• x: -0.0353</li> <li>• y: -0.0051</li> <li>• z: 0.9994</li> </ul>

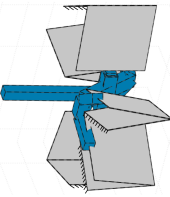
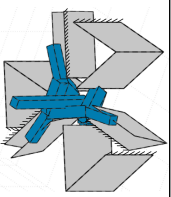
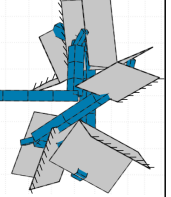
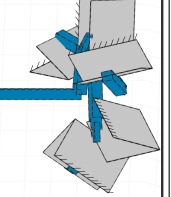
Continued on next page

Table D.1 – Continued from previous page

Concept	Figure	Thickness	Stress excl. warping	Stress incl. warping	Vibration modes incl. warping	Off centering
<b>6 leaf springs</b>		0.9 mm	383.08 MPa	672.68 MPa	<ol style="list-style-type: none"> <li>1. 1.52 Hz</li> <li>2. 20.03 Hz</li> <li>3. 40.82 Hz</li> </ol>	<ul style="list-style-type: none"> <li>• x: -0.0160</li> <li>• y: 0.1964</li> <li>• z: 0.9804</li> </ul>
<b>Butterfly</b>		0.8 mm	184.07 MPa	199.43 MPa	<ol style="list-style-type: none"> <li>1. 0.73 Hz</li> <li>2. 14.51 Hz</li> <li>3. 38.62 Hz</li> </ol>	<ul style="list-style-type: none"> <li>• x: 0.0012</li> <li>• y: 0.0032</li> <li>• z: 1.0000</li> </ul>
<b>Concept 1</b>		0.9 mm	276.24 MPa	486.81 MPa	<ol style="list-style-type: none"> <li>1. 1.25 Hz</li> <li>2. 20.92 Hz</li> <li>3. 21.14 Hz</li> </ol>	<ul style="list-style-type: none"> <li>• x: 0.0023</li> <li>• y: 0.0010</li> <li>• z: 1.0000</li> </ul>
<b>Concept 2</b>		Vertical: 0.6mm Horizontal: 0.9mm	427.57 MPa	761.82 MPa	<ol style="list-style-type: none"> <li>1. 1.44 Hz</li> <li>2. 21.14 Hz</li> <li>3. 21.98 Hz</li> </ol>	<ul style="list-style-type: none"> <li>• x: 0.0212</li> <li>• y: 0.0191</li> <li>• z: 0.9996</li> </ul>

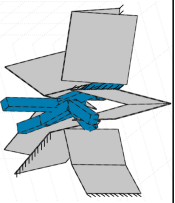
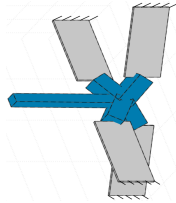
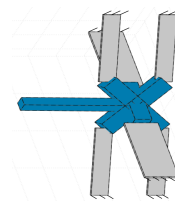
Continued on next page

Table D.1 – Continued from previous page

Concept	Figure	Thickness	Stress excl. warping	Stress incl. warping	Vibration modes incl. warping	Off centering
<b>Concept 2.2</b>		Vertical:1.2mm Horizontal:1.0mm	371.83 MPa	852.62 MPa	1. 1.79 Hz 2. 17.25 Hz 3. 21.12 Hz	<ul style="list-style-type: none"> <li>• x: -0.0018</li> <li>• y: -0.1358</li> <li>• z: 0.9907</li> </ul>
<b>Concept 2.3</b>		Vertical:0.6mm Horizontal:1.0mm	474.75 MPa	863.51 MPa	1. 1.27 Hz 2. 39.58 Hz 3. 40.37 Hz	<ul style="list-style-type: none"> <li>• x: -0.0037</li> <li>• y: -0.1755</li> <li>• z: 0.9845</li> </ul>
<b>Concept 3</b>		Vertical:0.9mm Angled:0.9mm	494.56 MPa	721.57 MPa	1. 2.21 Hz 2. 6.07 Hz 3. 17.13 Hz	<ul style="list-style-type: none"> <li>• x: 0.1304</li> <li>• y: 0.0199</li> <li>• z: 0.9913</li> </ul>
<b>Concept 3.2</b>		Vertical:1.0mm Angled:0.9mm	442.09 MPa	564.60 MPa	1. 2.10 Hz 2. 16.40 Hz 3. 18.65 Hz	<ul style="list-style-type: none"> <li>• x: -0.0448</li> <li>• y: -0.0331</li> <li>• z: 0.9984</li> </ul>

Continued on next page

Table D.1 – Continued from previous page

Concept	Figure	Thickness	Stress excl. warping	Stress incl. warping	Vibration modes incl. warping	Off centering
<b>Concept 4</b>		Vertical: 1.5 mm Horizontal: 0.9 mm	379.61 MPa	711.91 MPa	<ol style="list-style-type: none"> <li>2.14 Hz</li> <li>11.34 Hz</li> <li>20.48 Hz</li> </ol>	<ul style="list-style-type: none"> <li>x: -0.0041</li> <li>y: 0.1794</li> <li>z: 0.9838</li> </ul>
<b>Concept 7</b>		3.8 mm	5696.03 MPa	5695.01 MPa	<ol style="list-style-type: none"> <li>7.60 Hz</li> <li>23.76 Hz</li> <li>60.04 Hz</li> </ol>	<ul style="list-style-type: none"> <li>x: 0.0001</li> <li>y: 0.0000</li> <li>z: 1.0000</li> </ul>
<b>Concept 8</b>		4.2 mm	5811.25 MPa	5864.81 MPa	<ol style="list-style-type: none"> <li>8.49 Hz</li> <li>25.51 Hz</li> <li>65.70 Hz</li> </ol>	<ul style="list-style-type: none"> <li>x: 0.0000</li> <li>y: 0.0000</li> <li>z: 1.0000</li> </ul>

# E CONCEPT 1

## E.1 Optimization configuration

In this Appendix, the results of Second vibration mode for different configurations of concept 1 are shown.  $\alpha$  stands for the angle between the leafs of the folded leaf spring and  $\gamma$  for the angle between the folded leaf springs and the rotation line of the concept.

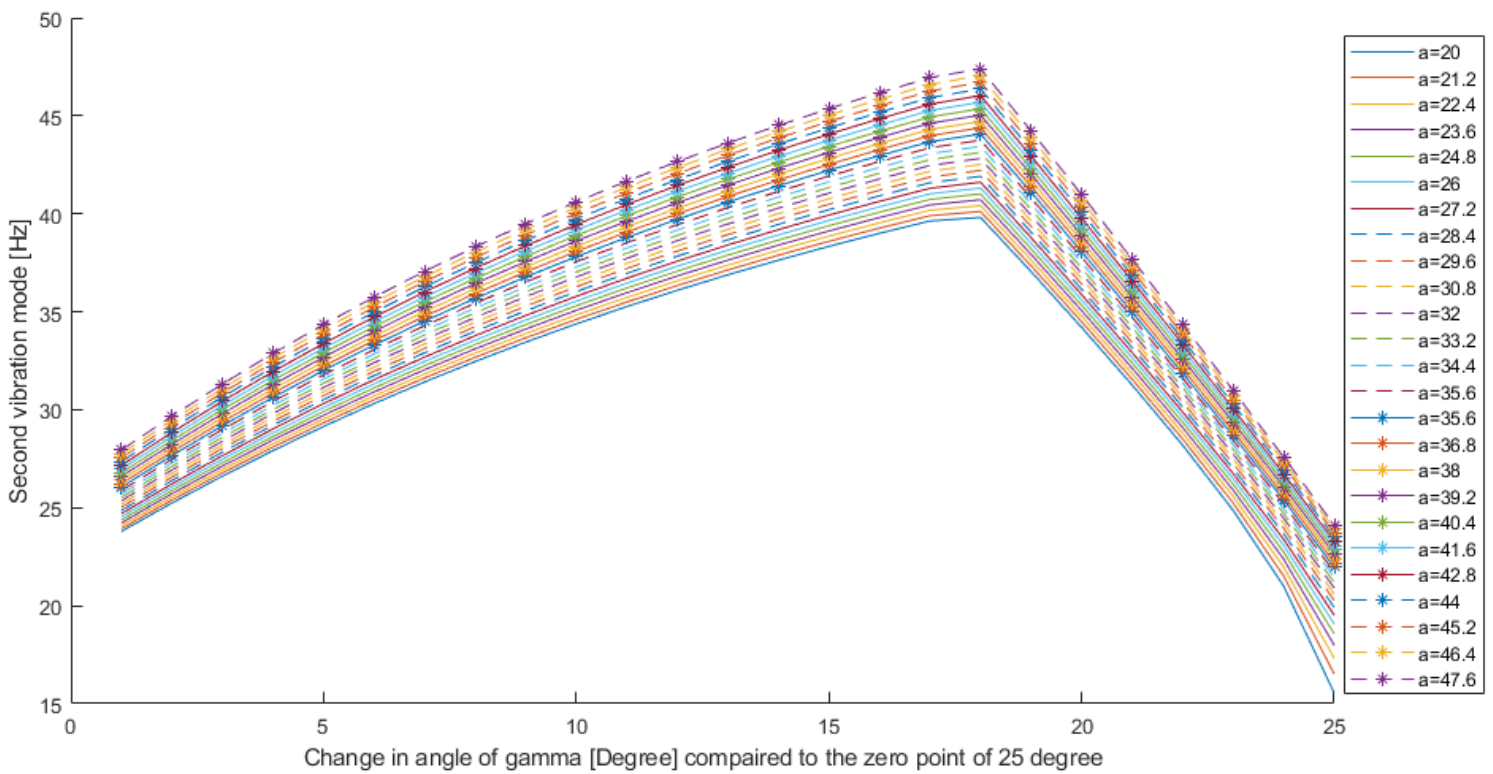


Figure E.1: Second vibration mode throughout a rotation around z for different configuration of flexures

## F 3 LEAF SPRING TORSION CONCEPT

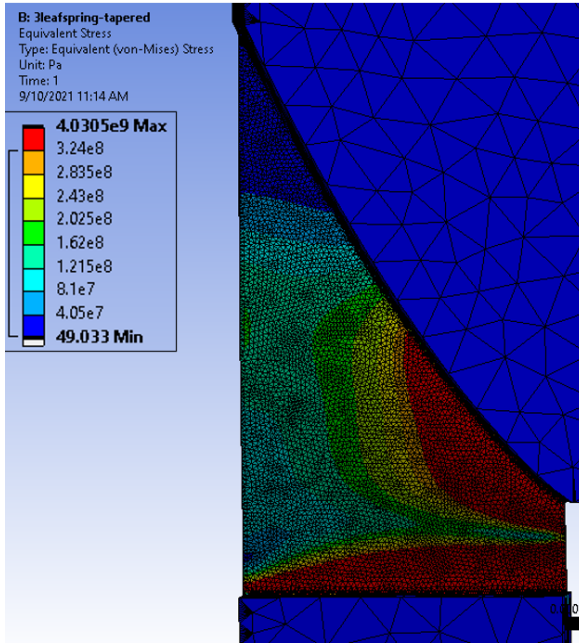
### F.1 Comparison between the different method of tapering

In this section, the comparison between three kinds of tapering is shown (parabolic tapered, conical on one side and conical on both sides). In most simulations, the models had very high local stress around the edges where the flexible and rigid parts are connected. The local high stress near the clamping can be neglected according to the saint Venant's principle. This principle states that local stress around a connection point will not influence the stress in the middle of the model [16]. Therefore, the stress at the connection edges can be altered by changing the connection between the rigid and flexible parts and can be neglected in these stress results.

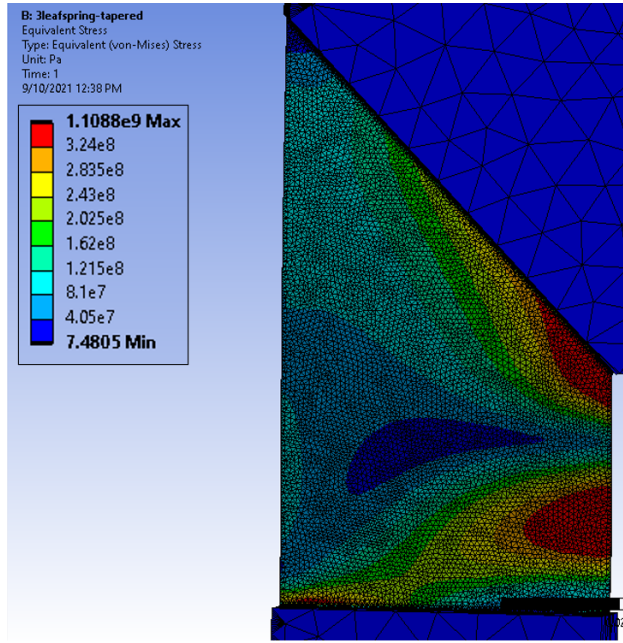
With the Spacar optimisations it is determined that smaller flexures will have lower stress than wide flexures. However, with smaller flexures the vibration modes are closer to each other and closer to the critical frequency of 30 Hz. To find the right middle ground between the stress level and vibration modes three different widths are investigated, 30 mm, 50 mm and 70 mm. For the different widths and 3 kind of tapering a stress analysis is performed in Ansys Workbench. The resulting stresses are given in the figures below.

The results show that the parabolic tapering does not give an equal distributed stress. In the top part of the tapering almost no stress is found, while the lowest part of the tapering has a high stress levels. When a one-sided conical shape is used the stress is distributed more evenly, but there is still low stress in the top point of the tapering. The most even distribution of stresses can be achieved when conical tapering is used on both sides of the flexure.

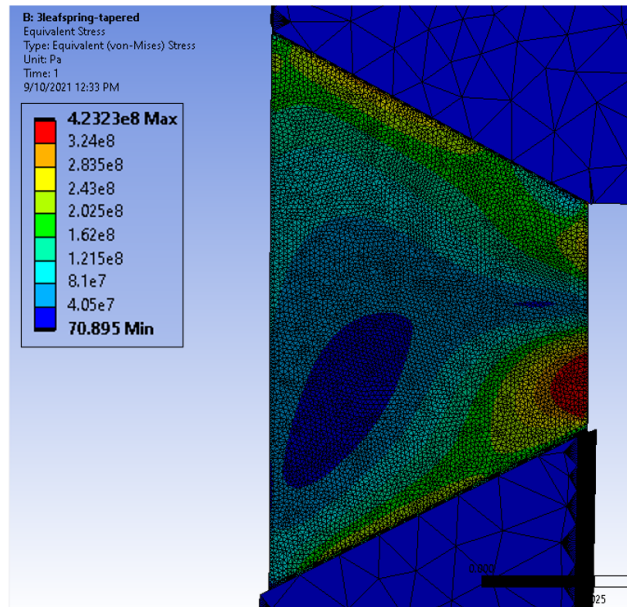
In Figure F.1c, can be seen that the parts where the stress is above the maximum allowed stress of 324 MPa, the red parts, are larger than just the connecting edges between the flexible and ridge parts. This means the stress with a rotation of  $\pm 5$  degree will be too high. While the stress for the 30 mm and 50 mm with an angle of  $\pm 5$  degree stays below the maximum stress of 324 MPa.



(a) Curved

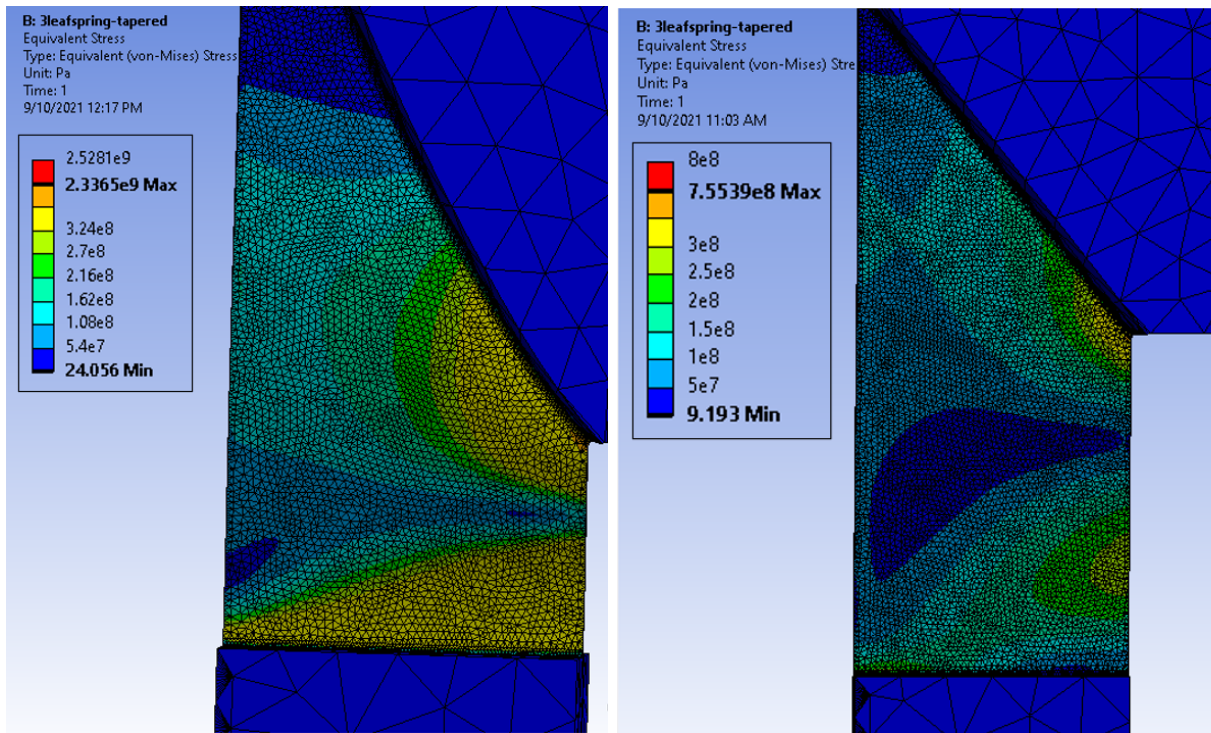


(b) Conical on one side



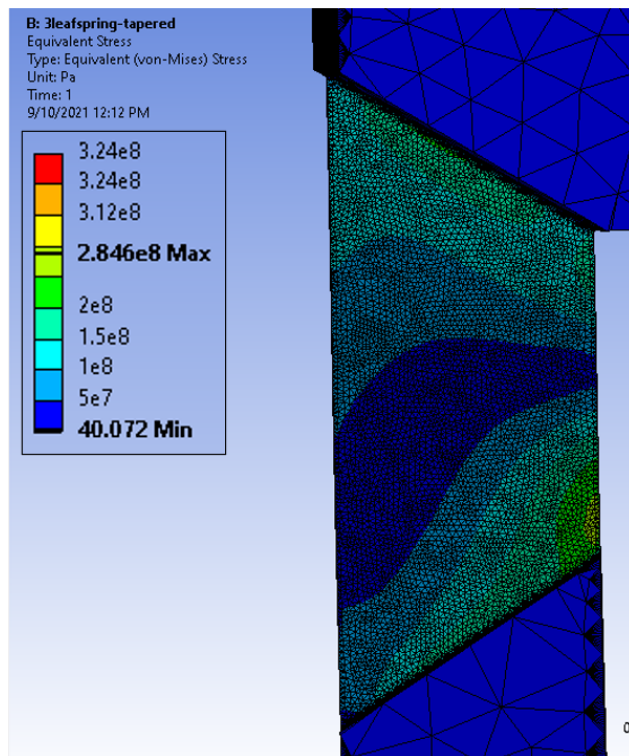
(c) Conical on both sides

Figure F.1: Three different kind of tapering for a width of 70 mm and a rotation of 5 degrees



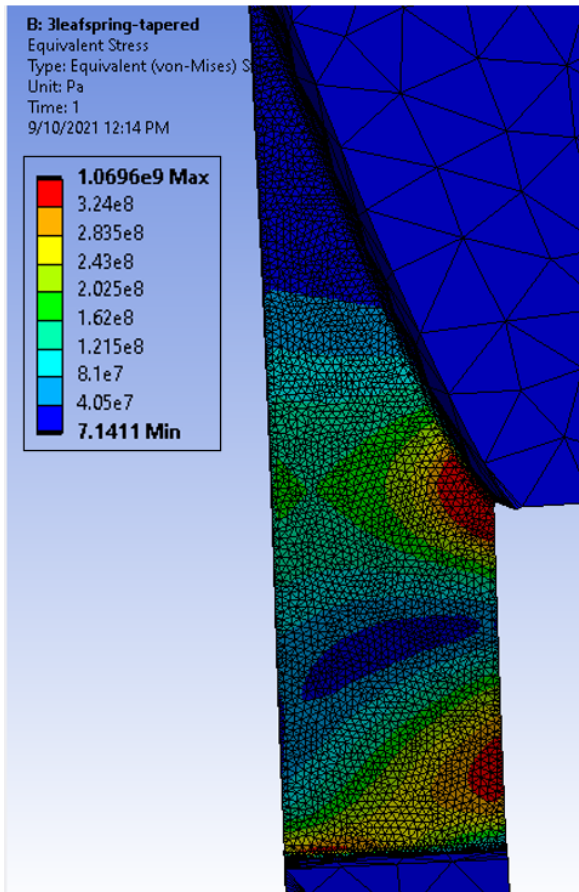
(a) Curved

(b) Conical on one side

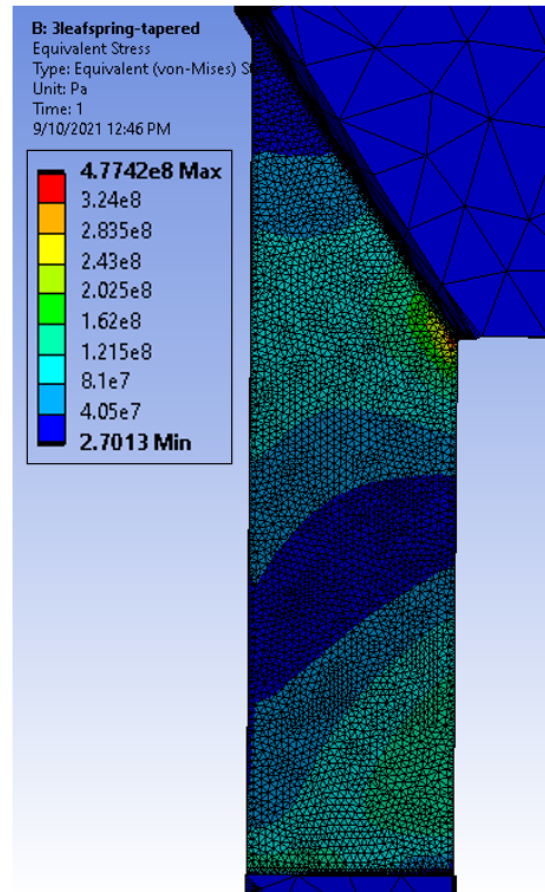


(c) Conical on both sides

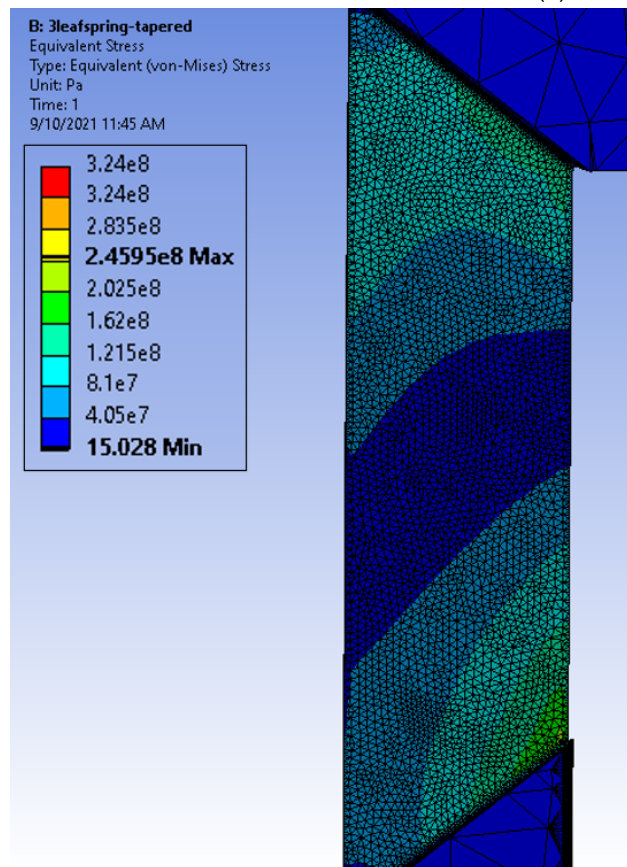
Figure F.2: Three different kind of tapering for a width of 50 mm and a rotation of 5 degrees



(a) Curved



(b) Conical on one side



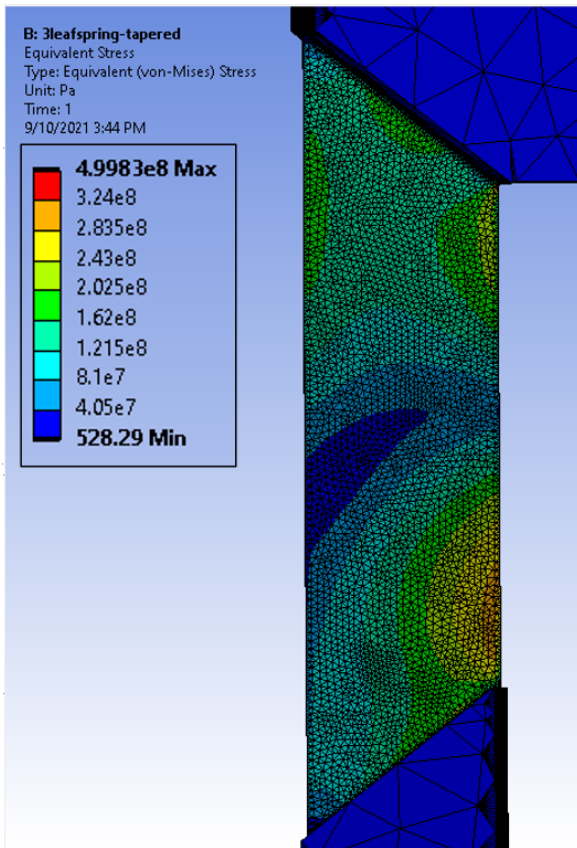
(c) Conical on both sides

Figure F.3: Three different kind of tapering for a width of 30 mm and a rotation of 5 degrees

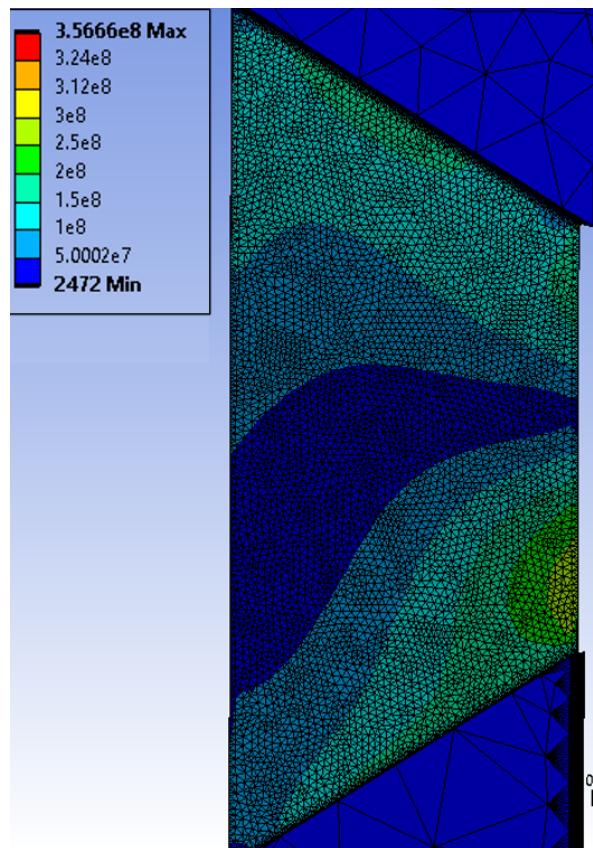
The model with 30 mm can do the largest angle,  $\pm 8$  degree, without exceeding the maximum stress, see Figure F.4. The 50 mm model maximum angle is  $\pm 6$  degrees. However, when the vibration modes are taken into account the 30 mm model does not fulfil the requirements of 30 Hz, see Table F.1. When a thicker flexure is considered the vibration modes are still not good. The second and third vibration modes are too low and the first mode becomes too high. While the 50 mm does have a good second vibration mode. The model with 50 mm has the best values for stress as well as vibration modes and is consequently chosen as the best possible solution.

Table F.1: Vibration modes Ansys Workbench 30 mm and 50 mm width

Width	Thickness	Vibration modes	Direction
30 mm	0.9 mm	1. 7.0901 Hz 2. 20.196 Hz 3. 20.199 Hz 4. 114.8 Hz	1. Rotation around z 2. Translation x 3. Translation y 4. Translation z
30 mm	2.0 mm	1. 22.833 Hz 2. 28.257 Hz 3. 28.264 Hz 4. 157.54 Hz	1. Rotation around z 2. Translation x 3. Translation y 4. Translation z
50 mm	0.9 mm	1. 11.125 Hz 2. 35.716 Hz 3. 35.728 Hz 4. 148.19 Hz	1. Rotation around z 2. Translation x 3. Translation y 4. Translation z



(a) Stress results of the 30 mm width model with a rotation of  $\pm 8$  degrees



(b) Stress results of the 50 mm width model with a rotation of  $\pm 6$  degrees

Figure F.4: Stress results of the 30 and 50 mm widths with their maximum rotation